A SURFACE MAGNETIC SURVEY

of

COSHOCTON COUNTY, OHIO

A Thesis

Presented in Partial Fulfillment of the

Requirements for the Degree, Bachelor of Science

by

Rodney A. Sheets Jr.

The Department of Geology and Minerology

Ohio State University

HONORABLE MENTION

1984

Approved by

Hallan C. Noltimier

Hallan C. Noltimier, Advisor
Department of Geology and Mineralogy

ABSTRACT

A total field magnetometer survey of nine quadrangles in Coshocton County is presented. The survey area is bounded by 40.125 and 40.500 degrees latitude and -81.617 and -82.000 degrees longitude. The anomaly field is derived from the total field values that are corrected for the IGRF and the diurnal fields. Corrected residual values are machine gridded at one half mile spacings, corresponding to 52 rows (latitude) and 43 columns (longitude). The grid node values were then machine contoured to produce anomaly maps of the area.

Two qualitative interpretations of the anomalies are given:

1.) Observed variations are due to basement faulting, or
2.) Observed variations are due to susceptibility and remanence variations across lithologic units.

ACKNOWLEDGEMENTS

I wish to thank Dr. Hallan Noltimier, my advisor, for suggesting this project, and for his support and assistance throughout this project.

Very special thanks go to Eric Cherry, With his kind help, this project got underway, progressed, and concluded.

Financial support for field work was provided by a grant from the Friends of Orton Hall.

TABLE OF CONTENTS

LIST OF FIGURES

LIST OF TABLES

1.0 INTRODUCTION

In eastern Ohio, little is known about local structure and lithology of the Precambrian basement complex. The only existing data are from sparse well control and recently completed aeromagnetic surveys. This surface magnetometer survey of Coshocton County, Ohio was undertaken for the purpose of learning more about the local structure and lithology of the basement.

This survey covered approximately 350 square miles, completely contained in Coshocton County, in east-central Ohio. A rectangular region bounded by 40.125 and 40.500 degrees latitude and -81.617 and -82.000 degrees longitude, was chosen to accomodate the 320 survey points and to serve as a basis for the gridding system used.

A grid spacing of one half mile was used. Previous aeromagnetic surveys are gridded at one mile. Higher resolution of the data is to be expected, due to the closer grid spacing and the lower elevation.

After corrections for the diurnal variations were performed, the total magnetic field at grid nodes was calculated. The International Geomagnetic Reference Field (IGRF) was then calculated at each survey point, and gridded at similiar spacing, and the values were subtracted from the total field values. The resulting residual values were interpreted qualitatively, because of the complexity of the data. Most magnetic modelling is variable and nonunique because it relies on many unknown

variables.

Two interpretations are presented:

1.) Observed variations are due to basement faulting, or

2.) Observed variations are due to susceptibility and remanence contrasts between lithologic units.

2.0 THEORETICAL BACKGROUND

To better understand the concepts and definitions of magnetics and the magnetic field, a brief review is appropriate.

The nature of the Earth's magnetic field has been established on the basis of world-wide measuements. The field is considered to be comprised of three components: (Nettleton, 1976)

1.) The main field comprises the largest proportion of the magnetic field observed at the surface of the Earth. This field arises due to convection currents in the liquid iron core of the Earth and follows a slow, but predictable secular change. (i.e. 'the westward drift')

2.) The smaller diurnal field behaves more erratically with time, but approximately follows a daily cycle. This field is due to electromagnetic currents in the upper atmospere and can be affected by magnetic storms, related to sunspots.

3.) The anomaly field is coused by magnetic inhomogeneities in the crust.

To evaluate the anomaly field with respect to lithologic changes in the crust, it must be separated from the effects of the main and diurnal fields.

2.1 Elements of the Main Field

The main field of the Earth can be separated into several components, each one defining a specific part of the field. F signifies the total intensity of the field, and H, the horizontal component of the field, along the magnetic meridian. The inclination or magnetic dip, I, is the angle between F and H, and the declination, D, is defined as the angle between H and geographic North. F, D, and I completely define the field at any point on the Earth's surface. (Jacob, 1963) These elements are shown vectorally by Figure 1.

2.2 Magnetic Field Variations

As stated above, variations in the field due to secular changes are slow. Isolation of anomalies, though, depend upon knowing what this field looks and acts like at the time of the survey. For this purpose, an International Geomagnetic Reference Field (IGRF) was adopted in 1965, to establish a uniformity to the field. This reference field is calculated assuming the Earth is a perfect sphere of magnetized material, which varies secularly and by locality. Every five years, a new IGRF is published, which contains coefficients for calculating the field's strength at any

place or time in the subsequent five years. The main magnetic field strength at the present time varies from 24,000 gammas at some places along the equator, to 68,000 gammas at the poles. In my survey area, the field strength averaged approximately 56,200 gammas.

If the Earth's field were measured continuously over a fixed point, it's intensity would change over time due to solar and lunar effects on the ionosphere. The solar effect is the larger of the two, and is seen when the survey is performed during the day. Determination of this variation is essential to define the nature of the field during a day's survey. Solar variations can reach up to 30 gammas, whereas lunar variations are usually 2 to 3 gammas.

Secular and diurnal variations are equally important when determining the nature of local anomalies.

2.3 Rock Magnetism

The magnetic moment of a rock body consists of two principal components, the remanant moment (M_R) and the induced moment (M_I). The remanant moment is the primary magnetization and is acquired by igneous and metamorphic rocks during cooling. The induced moment is the magnetization of the rocks in the present magnetic field.

The remanant moment is carried by the ferrimagnetic minerals, magnetite and hematite, which may comprise one to ten percent of the rock body. It's magnitude depends

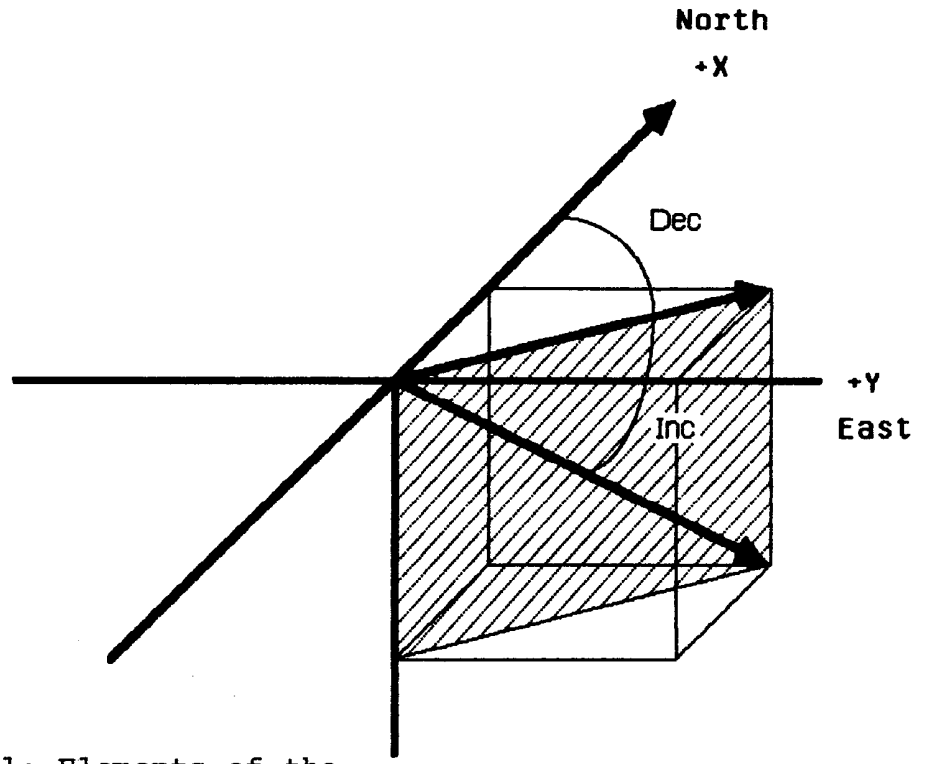

Figure 1: Elements of the Main Field

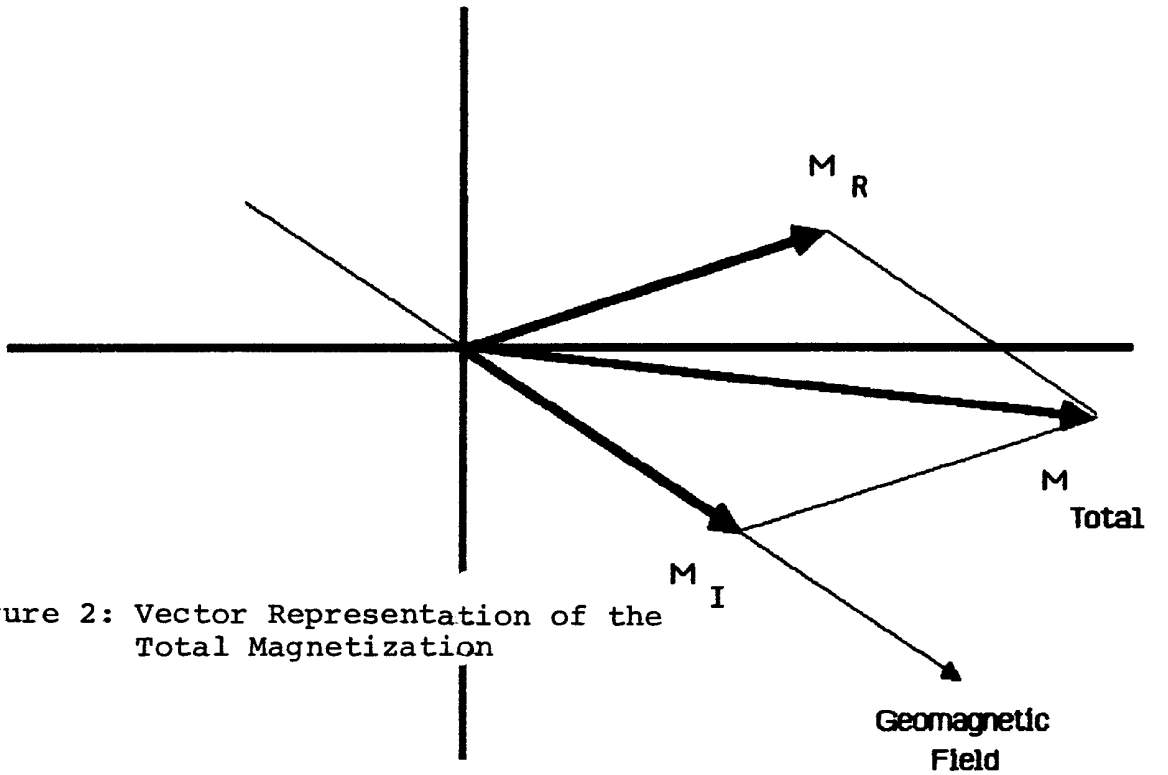

Figure 2: Vector Representation of the Total Magnetization

on the relative amounts and grain size of the magnetic phases. Remanence is acquired as the body cools through the Curie temperature of the minerals (580 C-680 C) and reflects the geomagnetic field at the time of cooling.

The induced moment reflects the magnetization of the rock body in the present geomagnetic field. This moment is directly related to the bulk magnetic susceptibility (k) of the rock, and the geomagnetic field strength, H, as given by the equation:

$$M_I = k*H$$

where k is the susceptibility in gauss/oerstead and H is the magnetic field strength in oerstead.

The susceptibility, k, is related to the amount of iron in the rock, including both the ferrimagnetic oxides and the ferromagnesium minerals.

Thus, the total magnetization, M_{Total}, is the vector sum of the remanant moment (M_R) and the induced moment, (M_I), as shown by Figure 2.

3.0 GEOLOGICAL AND GEOPHYSICAL STUDIES

3.1 Surface Geology

The Tuscararus and Walhoding Rivers empty into the Muskingum River valley, draining the survey area. Being just South of the glacial advance in Ohio, Illinoian glacial outwash fills the river basins and provides a groundwater reservoir, used extensively by the growing industrial

Figure 3: Lithologic Boundary (Lidiak, 1966)

Postulated basement fault (Zeitz, 1966)

Region structurally contoured (Figure 4)

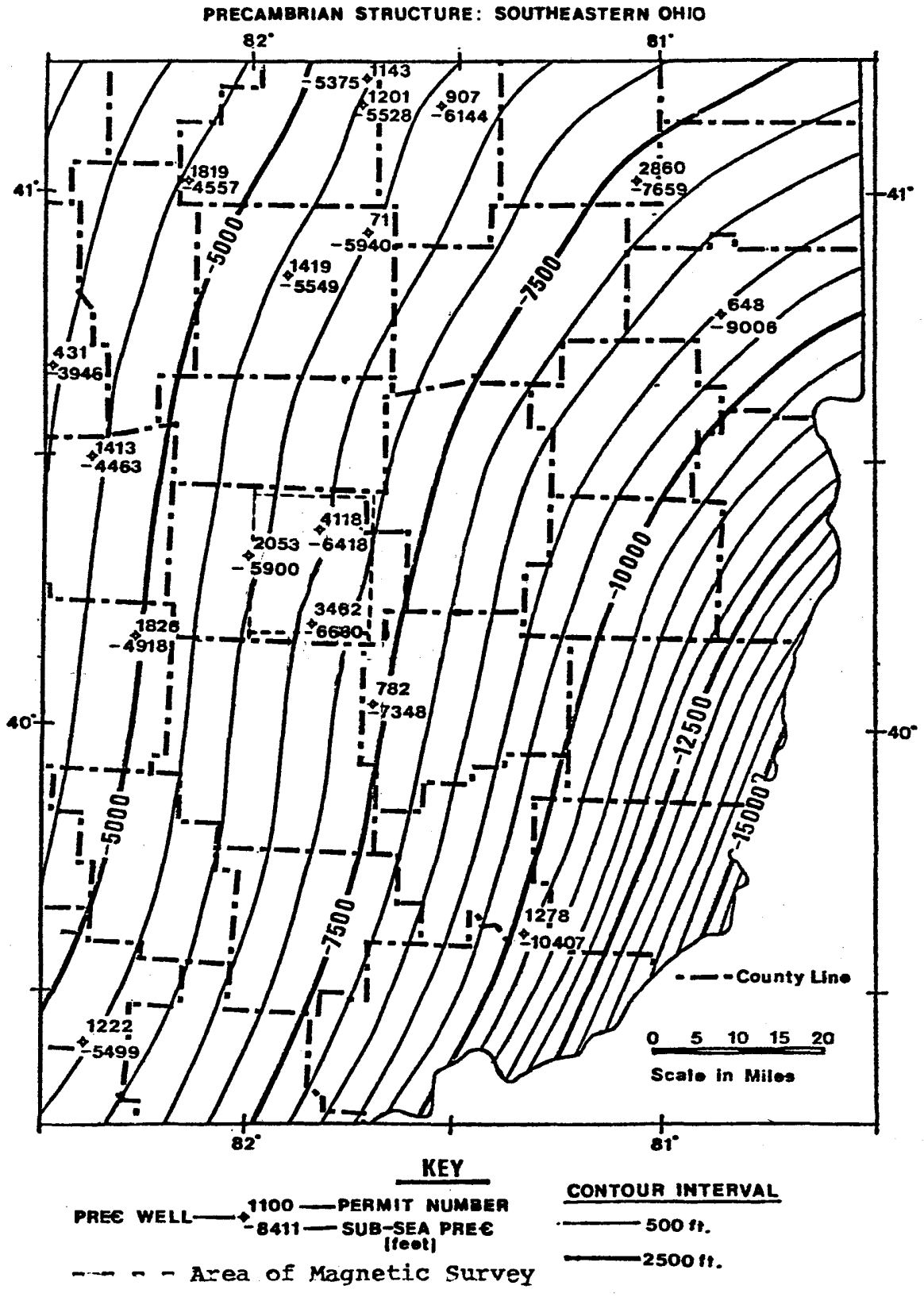

Figure 4: Modified after Rowan (1984)

cities of Coshocton and West Lafayette.

Pennsylavanian rocks, of the Allegheny and Pottsville groups, are predominately the surface rocks in the area, with varying lithologies. Sandstones persist, with shales and some limestones occurring, also. Just off the western edge of the survey area, iron-rich sandstones occur (Lamborn, 1954) that could affect a magnetometer survey. No such rocks are known to occur within the survey area. Coals are strip-mined extensively in the South-cental and South-eastern parts of the map area. Entrance into the mined area was possible, but measurements were restricted to proven map locations. Active mining areas were strictly forbidden, and as a result, gaps do exist in some parts of the maps.

3.2 Precambrian Geology

The precambrian rocks of Ohio are known only from sub-surface well data. From this data, a petrologic boundary is known to exist between older rhyolites and trachytes of western Ohio, and younger granites, granite gneisses, and monzonites of eastern Ohio. (Lidiak, et. al. 1966) (See Figure 3) East of this boundary, which is coincidental with the Findlay Arch, a basement structural high, the pre-cambrian surface dips to the east. Due to limited drill-ing data, only a general structure map can be produced, (See Figure 4) though several hundred feet of relief may exist in the form of erosional remnants. (Janssens, 1966)

In my survey area, the depth to the basement is approximated at 6000 feet on the western boundary, and 7000 feet in the East, by three wells recently drilled into the precambrian. Lithologies from these wells are shown in Table 1.

3.3 Geophysical Studies

Few geophysical studies have been attempted in eastern Ohio. Regional and statewide aeromagnetometer surveys have been done and a single gravimeter survey was done that covered parts of my survey area.

The most significant study related to my work was a regional aeromagnetometer survey, by Zeitz (1966), covering a continental strip between 38 and 41 degrees latitude, which included my survey area. In his report, he mentioned the possibility of a basement fault through central Coshocton County. The approximate trend of this proposed fault is shown in Figure 3.

A state aeromagnetic anomaly map, soon to be published, (von Frese, personal communication 1984) shows relatively quiet anomalies in the county, but a significantly low anomaly field, just to the west of the county.

Rowan (personal communication 1984) recently completed a gravimeter survey that included most of my map area. In it, he found North-east, South-west trending lineations, suspected to be of basement origin. Also, a gravity high was seen in the northwest corner of the map area, that may

TABLE 1

County	Permit Number	Depth to Precambrian (in feet below sea level)	Lithology
Coshocton	2053	-5900	Quartz Monzonite
	3462	-6680	----
	4118	-6416	Pegmatite*, gneiss, hornblende gneiss

* Pegmatite believed to be derived from basal arkose

TABLE 2*

Polarization Mechanism	Typical Polarization	Typical Susceptibility	Anistropy
Sedimentary rocks: DRM & PDRM, CRM	10^{-4} - 10^{-7} emu/cc	10^{-5}emu/ccOe	5%
	(For sedimentary iron cores, these values may be increased by an order of magnitude or more)		
Igneous rocks; TRM, CRM	10^{-2} - 10^{-4} emu/cc	10^{-2}-10^{-4}emu/ccOe	5-10%
Metamorphic rocks:	10^{-3} - 10^{-4} emu/cc	10^{-4}-10^{-5}emu/ccOe	5-25%

* Taken from (Noltimier, 1984)

also be controlled by the basement.

No other significant geophysical studies were completed in the survey area, though several other studies were completed in eastern Ohio, and not in the map area.

4.0 SURVEY PROCEDURE

This section takes up first, the general field procedures performed during my survey. The measurements necessarily include unwanted magnetic effects (the secular and diurnal field disturbances) and methods for their determination and removal are covered in the second part of this section.

4.1 Field Operations

4.1.1 Survey Technique

A major concern in the actual surface magnetic survey is the effect of diurnal variations. To better understand the nature of these variations, I used a 'looping' technique that required returning to a base station, or to a field station designated as a base, at regular time intervals. On the average, each loop consisted of between 8 and 10 field stations, which were in close proximity to the base station. At the end of each day, a diurnal variation curve was plotted, with field strength of the base and time as the y and x axes, respectively.

Most field station locations were subject to change, due to magnetic constraints. The stations were chosen beforehand, by road intersections and benchmarks, but

iron objects and electric wires, which affect the normal field, were often associated with these locations. Often, an offset of up to 200 yards was needed to eliminate their effects. Because of this, no measurements were made in the two major towns of Coshocton and West Lafayette.

4.1.2 The Magnetometer

For this surface magnetic survey, a Barringer Research Proton Precession Magnetometer was used, to measure the Earth's total field. (See Appendix 1) This magnetometer operates on the principal that protons will align themselves either parallel or perpindicular to any external magnetic field. When the external field is removed, the protons will return to their original direction (the Earth's field), by precessing around that field at a discrete angular velocity. To determine the total field, the frequency of the induced voltage, produced by this precession, is measured by counting the number of cycles of the precessional voltage and timing these cycles. (Dobrin, 1976)

4.2 Reduction of Data

4.2.1 Diurnal Corrections

As stated above, a primary concern in magnetic surveys is the effect of diurnal variations. The nature of this diurnal field was established through the 'looping'

method, as explained above, and for each day, a diurnal variation curve was plotted. (See Figure 5) Every day's values were added (or subtracted) to a normal value of 56,200 gammas, the average low value of the diurnal curves. This reduced the survey readings to a common reference point and corrected for the diurnal variation.

4.2.2 Total Field Correction

For this survey, a computer algorithm was obtained to calculate the International Geomagnetic Reference Field (IGRF) for each station location. (See Appendix 2 for program listing) The algorithm uses the 1980 IGRF coefficients and calculates the reference field at each station location, defined by latitude and longitude. A slight modification in the program yields the original field value, as corrected for diurnal variation, the IGRF value that corresponds to it, and residual value obtained by subtraction of the IGRF from the original value. Declinations and inclinations of each location are also computed.

4.2.3 Grid System

A rectangular grid, bounded by 40.125 and 40.500 degrees latitude and -81.617 and -82.000 degrees longitude, was placed over the original field values, the IGRF values, and the residual values. Fifty-two rows (latitude) and forty-three columns (longitude) resulted

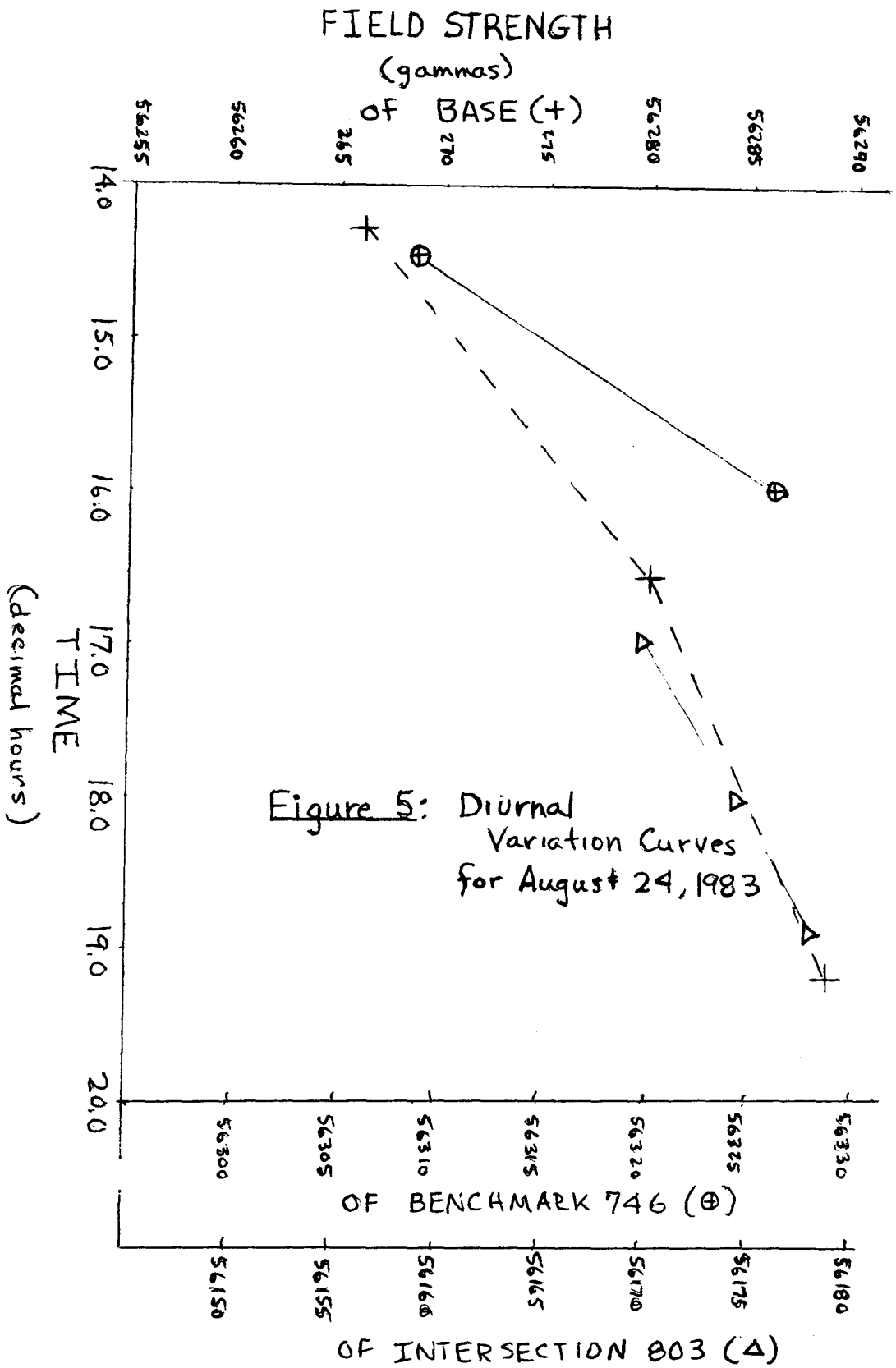

Figure 5: Diurnal Variation Curves for August 24, 1983

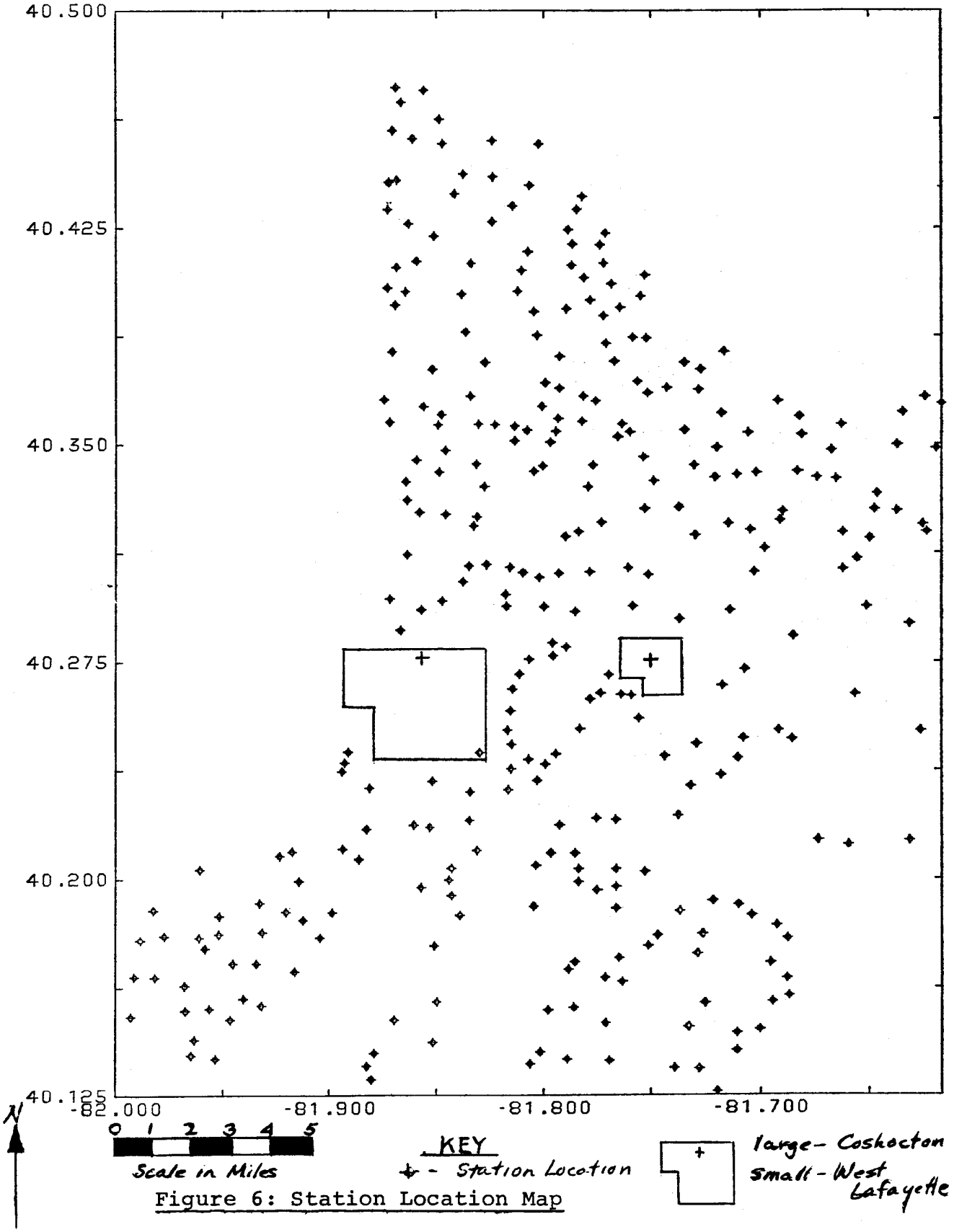

Figure 6: Station Location Map

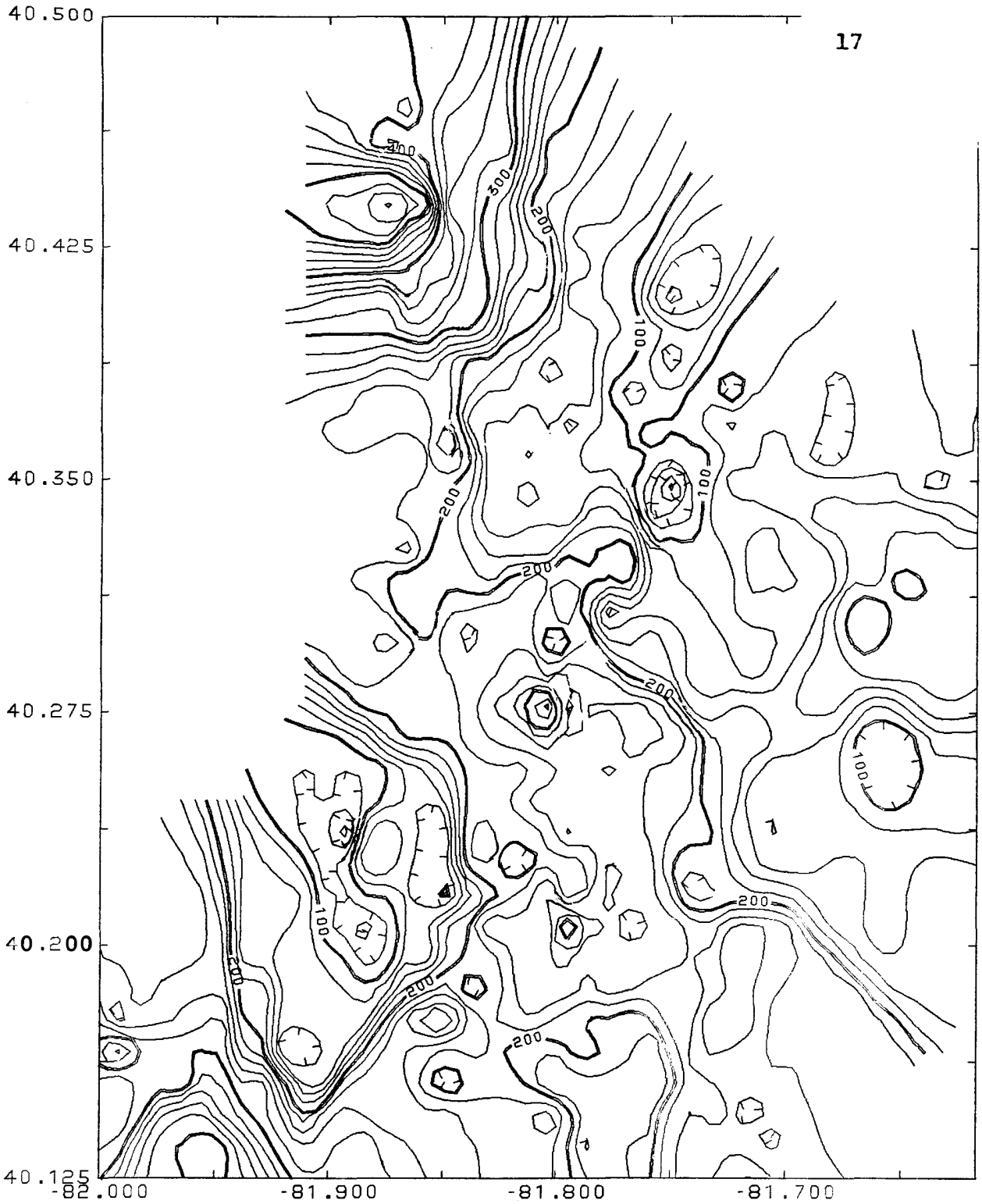

Figure 7: Contour Map of Original Field Values
(CI= 20 gammas)

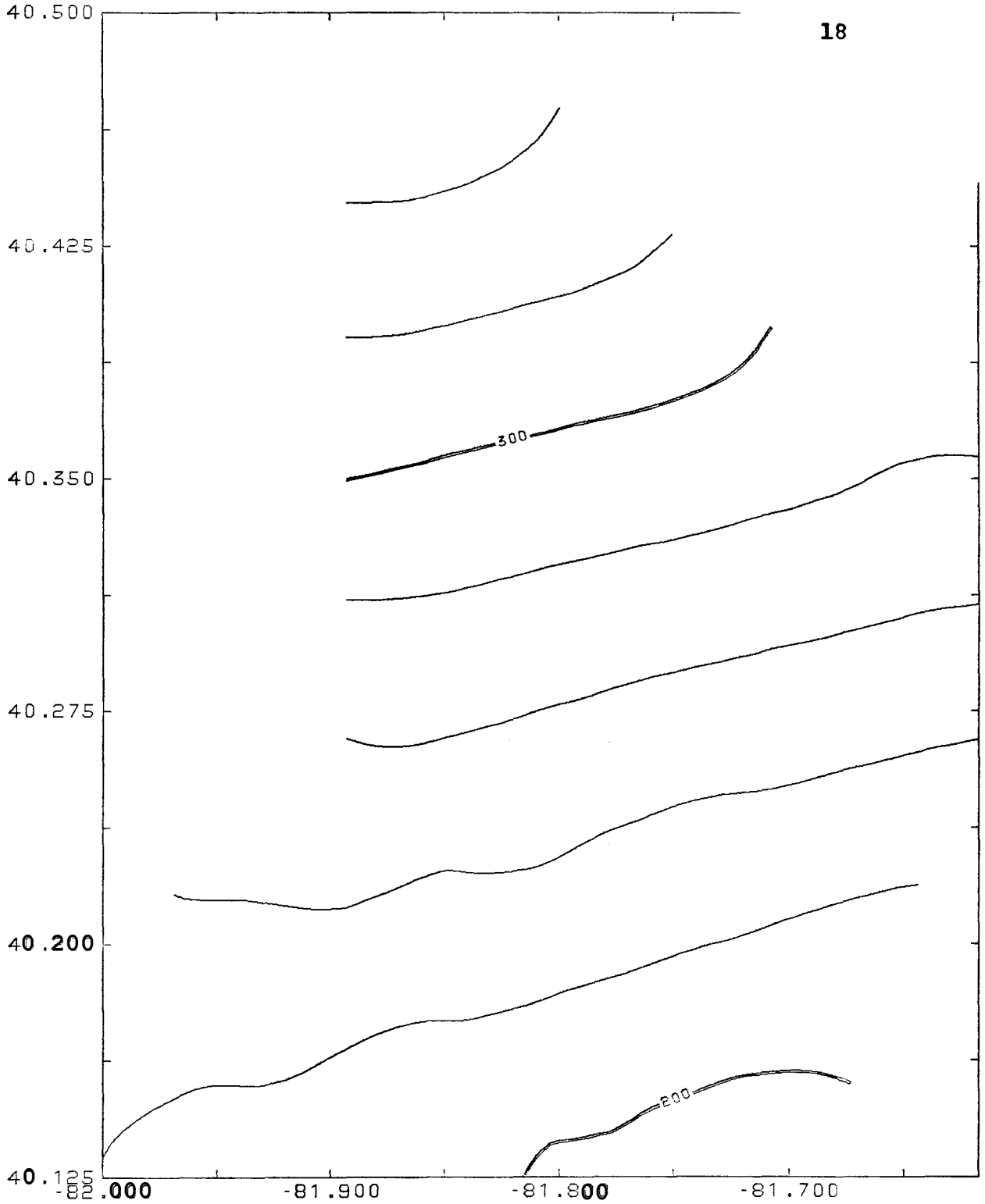

Figure 8: Contour Map of IGRF values
(CI= 20 gammas)

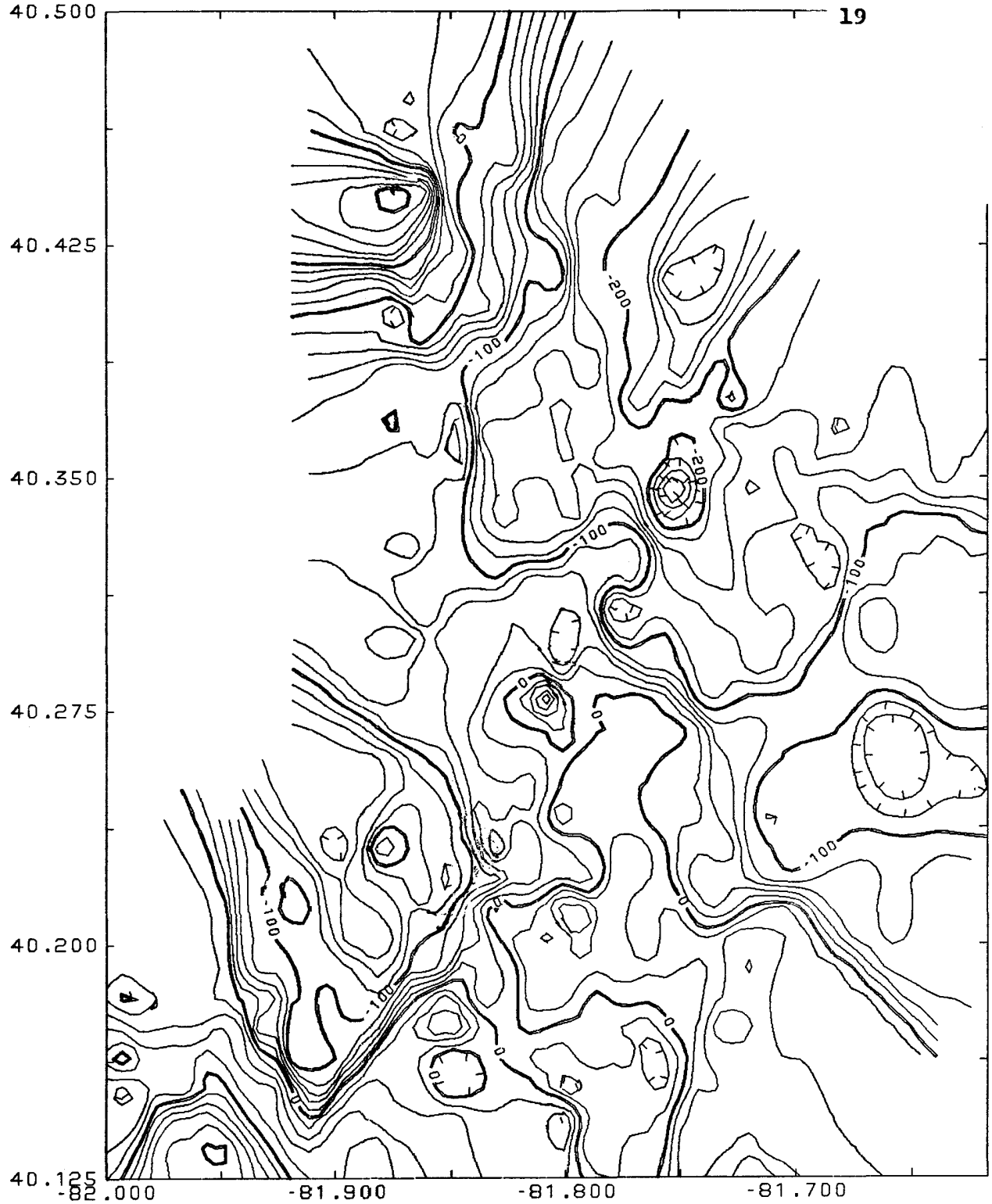

Figure 9: Contour Map of Residual Values
(CI= 20 gammas)

in a grid spacing of one half mile. The grid nodes were calculated using a nearest eight neighbor approximation, with one over the distance to the points, as the weighting parameter. (Surface II Graphics, 1976) The grid points were machine contoured with Bessel function smoothing.

The original survey point locations are shown in Figure 6, with the contour maps of the original total field values, the IGRF field values, and the residual values shown in Figures 7,8, and 9, respectively. Block diagrams of each set of values are shown in plates 1,2, and 3, respectively.

5.0 RESULTS AND INTERPRETATION

Residual values were obtained by subtracting the IGRF values from the corrected field values. These residuals are shown in Appendix 3. The values were gridded and contoured (as above) to obtain the anomaly map in Figure 9.

Potential field data (gravity and magnetics) is affected by many variables whose parameters are not always known. In magnetic interpretation, one interprets a situation as if it were geologically simple, to control variables that are unknown. Many times, a situation can be resolved using different interpretations. Because of this nonuniqueness of interpreting anomalies, a complex area, such as this one, can be interpreted in many ways, which may be equally correct.

Before interpretation of the anomalies, a background of

remanence effects is given, to serve as a basis for the interpretation. Because of the magnetic complexity of the region, two qualitative interpretations are presented:

1.) Observed variations are due to basement faulting, or

2.) Observed variations are due to susceptibility and remanence contrasts between lithologic units.

5.1 Effects of Remanence on Interpretation

The thick sedimentary cover in eastern Ohio is transparent in magnetics, due to susceptibility and remanence differences between the sediments and the igneous or metamorphic basement rocks. The total magnetic field is wholely controlled by structural events in the basement, or by the basement rocks themselves. Typical polarizations and susceptibilities, shown in Table 2, indicate that sediments are virtually nonexistent, magnetically speaking.

The precambrian rocks of eastern Ohio are known to be of the Grenville Province, whose apparent polar wander curve (APW) indicates that it was at, or close to, the equator at the time of its formation, one billion years ago. (See Figure 10) This information suggests that the remanant polarization of the basement in my survey area is approximately East-West. This polarization will accentuate anomalies associated with thin slabs (faults) in the basement, and with changes of lithology, across the basement.

5.2 Interpretation 1-- Faulting

Upon inspection of the anomaly map (Figure 9), a pair

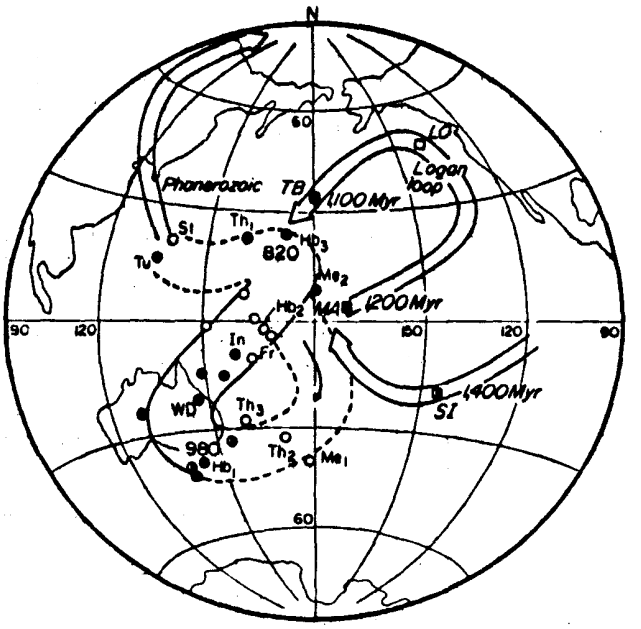

Figure 10: Proposed Grenville Apparent Polar Wander Curve (Berger, et. al. 1976)

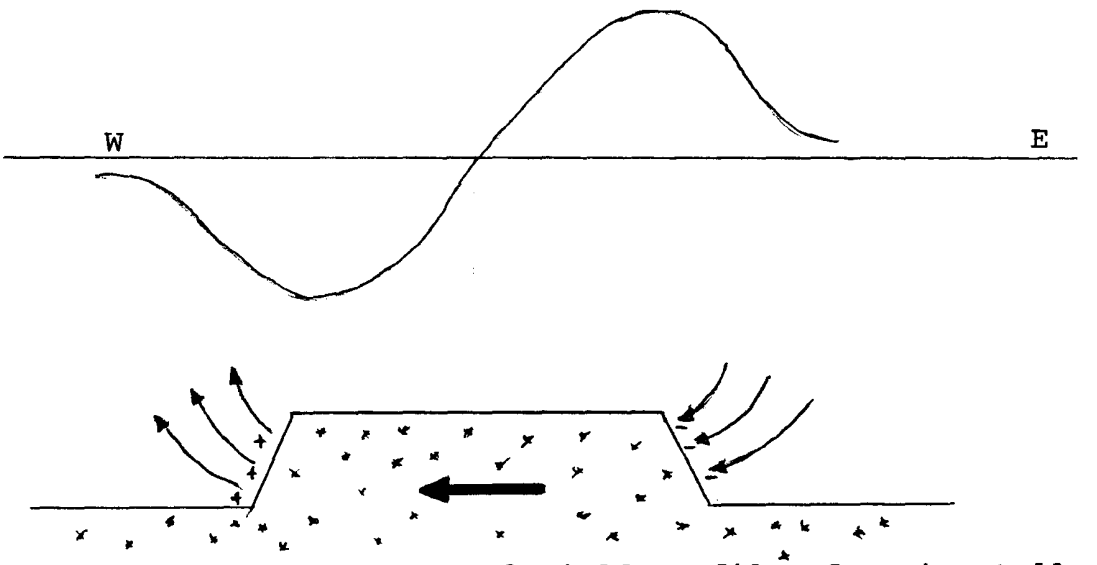

Figure 12: Total Field Profile of Horizontally Polarized Fault Block

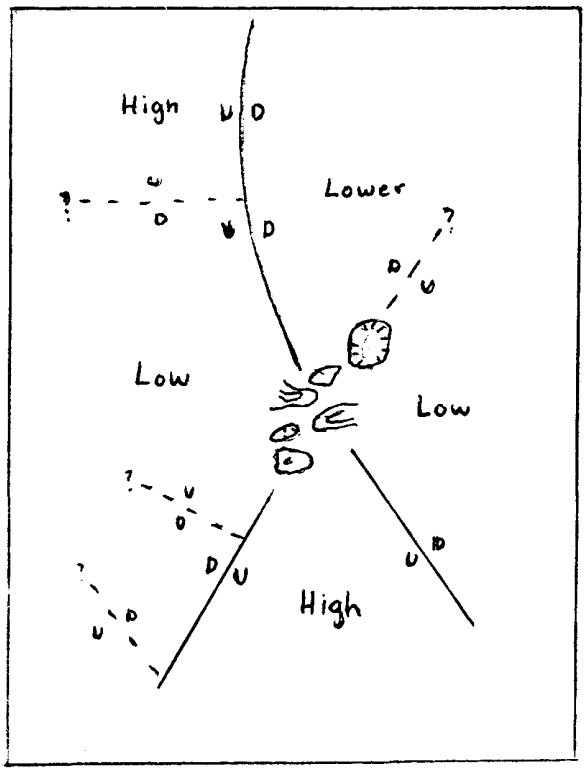

Figure 11: Fault Interpretation for Anomalies

(Solid lines represent lineations interp. by faults--dashed refer to anomaly changes that may be due to faults)

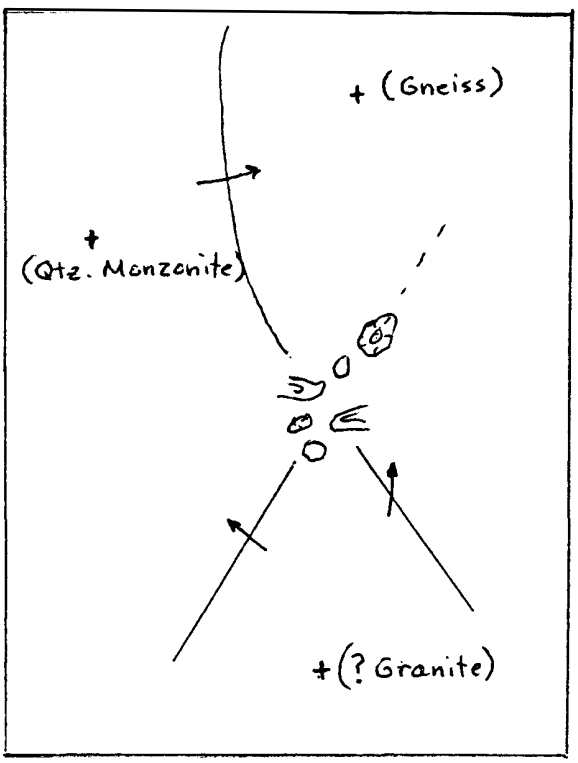

Figure 13: Lateral Lithology Variation Interpretation

(Solid lines represent lineations interp. by lithological boundaries-Arrows point to lithology of lower susceptibility)

of lineations is seen; one that trends northeast-southwest (NE-SW) and a second that trends northwest-southeast (NW-SE). (See Figure 11) Associated with the first, and most prominent, lineation are small negative and positive anomalies of up to 2 mile in diameter. As they are controlled by 3 or more data points, it is unlikely they are spurious anomalies. Their position along the lineation leads me to believe that they could be a result of faulting and subsequent remineralization or alteration of magnetic minerals. In a paper by Henkel and Guzman (1977), the oxidation of magnetite to hematite along fracture zones was associated with local magnetic minima. This is possibly applicable to this situation.

Upon observation of the NE-SW lineation, one sees a general decrease in anomaly values from East to West, of about 100 gammas. The NW-SE lineation exhibits a decrease of a similiar amount, from West to East. A horizontally polarized fault block exhibits anomalies that could be assimilated to this situation. (See Figure 12) A high anomaly field is associated with the negative pole, or the eastern edge of the block. A low anomaly field is coincident with the positive pole, or the western edge of the block. Figure 11 shows the general structure that could produce the anomalies seen in my survey area. The faults are drawn essentially vertical to produce sufficient relief.

5.3 Interpretation 2-- Lateral Susceptibility and Remanence Variations

Changes in lithology which give rise to lateral contrasts in susceptibility show up in the magnetic contours more readily than topographic features on the basement. (Dobrin, 1976)

In this survey area, the magnetic contours produced can be interpreted as lateral variation of lithology; hence, susceptibility. The three well logs in the area indicate that a noticeable change of lithology occurs. (See Table 1) In the western part of the survey area, a quartz monzonite basement exists, and in the northeast a gneissic one. These two different lithologies may indicate a significant change in susceptibility, which will cause a change in the character of anomalies produced.

The lineations described above, may just as well be interpreted as a contact between basement rocks of differing lithologies and susceptibilities. In Figure 13, possible lithologic regions are shown that may account for the anomaly lineations and the change in appearance of the anomaly fields.

6.0 CONCLUSIONS AND RECOMMENDATIONS

The magnetic anomaly map of Coshocton County, Ohio is complicated. Two qualitative interpretations of the area are:

1.) Observed variations are due to basement faulting, or

2.) Observed variations are due to susceptibility and remanence contrasts between lithologic units.

Further studies could better determine the nature of the body producing the anomalies. Three further analyses of the data that could increase the amount of processable information are:

1.) Reduction to the Pole
2.) Frequency Filtering
3.) Upward Continuation

Reduction to the pole procedures makes it possible to determine, from the observed total field, the position and depth of the pole that has a magnetic effect equivalent to that of an extended source with inclined magnetization. (Dobrin, 1976) This technique involves separating the field into its symmetric and antisymmetric parts and can be implemented through the use of algorithms written just for this purpose.

Frequency filtering and upward continuation both result in smoothing of the resulting magnetic contours. Upward continuation is sometimes used to simplify the appearance of magnetic maps, by suppressing local features. Frequency filtering removes undesired signals (noise) from the area, leaving primary frequencies, which are important in interpreting. These are also easily implemented by computer programs.

REFERENCES

Barringer Research Limited, Operation Manual, Ground Magnetometer Model GM-122, Toronto, Canada, 10 pp.

Berger, G. W., York, D. and Dunlop, D. J., 1979, Calibration of Grenvillian paleopoles by $^{40}A/^{39}Ar$ dating. Nature 277, pp. 46-48.

Dobrin, M., 1976, Geophysical Prospecting, New York, McGraw-Hill, pp. 509-512.

Henkel, H., Guzman, M., Magnetic features of fracture zones. Geoexploration 15, 1977, pp. 173-181.

Jacob, J. A., "The Earth's Core and Geomagnetism", The Macmillan Company, pp. 45-48, 1963.

Janssens, A., 1973, Stratigraphy of the Cambrian and lower Ordovician rocks of Ohio. Ohio Geol. Surv. Bull. 64, pp. 197.

Landorn, R. A., Geology of Coshocton County. Geol. Soc. of Amer. Bull., 1954, pp. 10-12.

Lidiak, E. G., Marvin, R. F., Thomas, H. H., and Bass, M. N., 1966, Geochronology of the Midcontinent Region, United States: No. 4 eastern area. Jour. of Geophy. Res., v. 71, no. 12, pp. 1427-1448.

Nettleton, L. L., "Geophysical Prospecting for Oil", McGraw-Hill. New York, 1976.

Noltimier, H. C., Paleomagnetism Seminar notes: G&M 820, The Ohio State University, 1984.

Rowan, D. J., Personal Communication- Gravity Survey of Coshocton County, The Ohio State University, 1984.

Surface II Graphics, Manual, Kansas State Geological Survey, 1976, 250 pp.

von Frese, R. R. B., Personal Communication-Future publication of Ohio aeromagnetic maps by O.G.S and U.S.G.S., The Ohio State University, 1984

Zeitz, I., King, E. R., Geddes, W., and Lidiak, E. G., 1966, Crustal Study of a continental strip from the Atlantic Ocean to the Rocky Mountains. Geol. Soc. Amer. Bull., v. 77, no. 12, pp. 1045-1048.

APPENDICES

APPENDIX 1: MAGNETOMETER SPECIFICATIONS

SPECIFICATIONS

Range:	20,000 to 99,999 in 12 ranges
Accuracy:	± 1 γ through operating temperature range
Sensitivity:	1 γ
Gradient Tolerance:	600 γ/ft.
Power:	12 "D" cells
Power Consumption:	< 50 Joules (Wsec) per reading
Polarizing Power:	0.8 @ 13.5 V for 1.5 sec. (3 second cycle) 0.8 A @ 13.5 V for 3 sec. (6 second cycle)
Number of Readings with 1 Battery Set:	2,000 - 10,000 depending on type of batteries
Frequency of Readings:	1 every 3 seconds 1 every 6 seconds
Controls:	Pushbutton switch Range Selection switch - Slide switch for 3 and 6 sec. located on P/C Board
Output:	5 digit incandescent filament readout
Indicators:	LED point Lock Indicator - last three digits of the display blanked off when phaselock not achieved Segment Function Indicator - all segments light up to permit visual inspection of the display function

APPENDIX 2: PROGRAM GEOMAG

with

1980 IGRF coefficients

```
1.      // JOB
2.      /*JOBPARM LINES=2000
3.      // EXEC PLOTV
4.      //GO.SOURCE   DD *
5.      C
6.      C
7.      C       THIS PROGRAM CALCULATES THE IGRF FIELD AT ANY POINT, USING
8.      C       THE MOST RECENT IGRF COEFFICIENTS (1980).  IT ALSO CALCULATES
9.      C       THE DIFFERENCE BETWEEN THE MEASURED FIELD AND THE IGRF (DIFF)
10.     C       AND THE DECLINATION (DEC) AND INCLINATION (INC) OF THE FIELD
11.     C       AT THE POINT.
12.     C
13.             IMPLICIT REAL*8(A-H,O-Z)
14.             REAL*8 INC(50),DEC(50)
15.             ELV=0
16.             LL=1
17.             CALL FIELDG (0.,0.,0.,0.,18,LL,Q1,Q2,Q3,Q4)
18.             DO 10 I=1,322
19.             READ (5,90) YEAR,APHI,ATHETA,F1
20.             CALL FIELDG (ATHETA,APHI,ELV,YEAR,50,LL,X,Y,Z,FF)
21.             H=DSQRT(X**2+Y**2)
22.             INC(J)=DATAN(Z,H)
23.             DEC(J)=DATAN(Y,X)
24.             PI=4.00*ATAN(1.00)/180.00
25.             INC(J)=INC(J)/PI
26.             DEC(J)=DEC(J)/PI
27.             DIFF=F1-FF
28.             WRITE (6,91) YEAR,APHI,ATHETA,F1,FF,DIFF,INC(J),DEC(J)
29.          10 CONTINUE
30.          90 FORMAT (2X,F7.2,1X,F8.4,2X,F7.4,2X,F7.1)
31.          91 FORMAT (2X,F7.2,1X,F8.4,2X,F7.4,3(2X,F7.1),2(5X,F7.4))
32.             STOP
33.             END
34.           SUBROUTINE FIELDG (DLAT,DLONG,ALT,TM,NMX,L,X,Y,Z,F)
35.     C
36.     C
37.     C       ****************************************************************
38.     C       FOR DOCUMENTATION OF THIS SUBROUTINE AND SUBROUTINE FIELD SEE :
39.     C            NATIONAL SPACE SCIENCE DATA CENTER*S PUBLICATION
40.     C            **COMPUTATION OF THE MAIN GEOMAGNETIC FIELD
41.     C              FROM SPHERICAL HARMONIC EXPANSIONS**
42.     C            DATA USERS' NOTE, NSSDC 68-11, MAY 1968
43.     C            GODDARD SPACE FLIGHT CENTER, GREENBELT, MD.
44.     C       ****************************************************************
45.     C
46.     C        DLAT ** LATITUDE IN DEGREES POSITIVE NORTH
47.     C       DLONG ** LONGITUDE IN DEGREES POSITIVE EAST
48.     C         ALT ** ELEVATION IN KM (POSITIVE ABOVE, NEGATIVE BELOW
49.     C                EARTH'S SURFACE)
50.     C          TM ** EPOCH IN YEARS
51.     C         NMX ** SET TO INTEGER GREATER THAN DEGREE OF EXPANSION
52.     C           L ** SET TO 1 ON INITIAL DUMMY CALL, SET TO 0 ON SUBSEQUENT
53.     C                CALLS
54.     C
55.     C       SUBROUTINE RETURNS GEOMAGNETIC FIELD DIRECTIONS (X,Y,Z), POSI-
56.     C       TIVE NORTH, EAST AND DOWN, RESPECTIVELY, AND MAGNITUDE OF TOTAL
57.     C       FIELD, F---ALL VALUES ARE IN GAMMAS
58.     C
59.     C
```

```
      EQUIVALENCE (SHMIT(1,1),TG(1,1))
      COMMON /NASA/ TG(18,18)
      COMMON /FLDCOM/ ST,CT,SPH,CPH,R,NMAX,BT,BP,BR,B
      DIMENSION G(18,18), GT(18,18), SHMIT(18,18), AID(11), GTT(18,18)
      DATA A/0./
C
      TLAST=0.0
C
      IF(A.EQ.6378.16) IF(L) 210,100,110
C
      A=6378.16
      FLAT=1.-1./298.25
      A2=A**2
      A4=A**4
      B2=(A*FLAT)**2
      A2B2=A2*(1.-FLAT**2)
      A4B4=A4*(1.-FLAT**4)
      IF (L) 160,160,110
  100 IF (TM-TLAST) 190,210,190
  110 READ (3,260) J,K,TZERO,(AID(I),I=1,11)
      L=0
      WRITE (6,270) J,K,TZERO,(AID(I),I=1,11)
      MAXN=0
      TEMP=0.
  120 READ (3,280) N,M,GNM,HNM,GTNM,HTNM,GTTNM,HTTNM
      IF (N.LE.0) GO TO 130
      MAXN=(MAX0(N,MAXN))
      G(N,M)=GNM
      GT(N,M)=GTNM
      GTT(N,M)=GTTNM
      TEMP=AMAX1(TEMP,ABS(GTNM))
      IF (M.EQ.1) GO TO 120
      G(M-1,N)=HNM
      GT(M-1,N)=HTNM
      GTT(M-1,N)=HTTNM
      GO TO 120
  130 WRITE (6,290)
      DO 150 N=2,MAXN
      DO 150 M=1,N
         MI=M-1
         IF (M.EQ.1) GO TO 140
         WRITE (6,300) N,M,G(N,M),G(MI,N),GT(N,M),GT(MI,N),GTT(N,M),GTT(
     1   MI,N)
         GO TO 150
  140    WRITE (6,310) N,M,G(N,M),GT(N,M),GTT(N,M)
  150 CONTINUE
      WRITE (6,320)
      IF (TEMP.EQ.0.) L=-1
  160 IF (K.NE.0) GO TO 190
      SHMIT(1,1)=-1.
      DO 170 N=2,MAXN
         SHMIT(N,1)=SHMIT(N-1,1)*FLOAT(2*N-3)/FLOAT(N-1)
         SHMIT(1,N)=0.
         JJ=2
      DO 170 M=2,N
         SHMIT(N,M)=SHMIT(N,M-1)*SQRT(FLOAT((N-M+1)*JJ)/FLOAT(N+M-2))
         SHMIT(M-1,N)=SHMIT(N,M)
  170 JJ=1
      DO 180 N=2,MAXN
      DO 180 M=1,N
```

```
120.                G(N,M)=G(N,M)*SHMIT(N,M)
121.                GT(N,M)=GT(N,M)*SHMIT(N,M)
122.                GTT(N,M)=GTT(N,M)*SHMIT(N,M)
123.                IF (M.EQ.1) GO TO 180
124.                G(M-1,N)=G(M-1,N)*SHMIT(M-1,N)
125.                GT(M-1,N)=GT(M-1,N)*SHMIT(M-1,N)
126.                GTT(M-1,N)=GTT(M-1,N)*SHMIT(M-1,N)
127.          180 CONTINUE
128.          190 T=TM-TZERO
129.              DO 200 N=1,MAXN
130.              DO 200 M=1,N
131.                 TG(N,M)=G(N,M)+T*(GT(N,M)+GTT(N,M)*T)
132.                 IF (M.EQ.1) GO TO 200
133.                 TG(M-1,N)=G(M-1,N)+T*(GT(M-1,N)+GTT(M-1,N)*T)
134.          200 CONTINUE
135.              TLAST=TM
136.          210 DLATR=DLAT/57.2957795
137.              SINLA=SIN(DLATR)
138.              RLONG=DLONG/57.2957795
139.              CPH=COS(RLONG)
140.              SPH=SIN(RLONG)
141.              IF (J.EQ.0) GO TO 220
142.              R=ALT+6371.0
143.              CT=SINLA
144.              GO TO 230
145.          220 SINLA2=SINLA**2
146.              COSLA2=1.-SINLA2
147.              DEN2=A2-A2B2*SINLA2
148.              DEN=SQRT(DEN2)
149.              FAC=(((ALT*DEN)+A2)/((ALT*DEN)+B2))**2
150.              CT=SINLA/SQRT(FAC*COSLA2+SINLA2)
151.              R=SQRT(ALT*(ALT+2.*DEN)+(A4-A4B4*SINLA2)/DEN2)
152.          230 ST=SQRT(1.-CT**2)
153.              NMAX=MIN0(NMX,MAXN)
154.       C
155.              CALL FIELD
156.       C
157.              Y=BP
158.              F=B
159.              IF (J) 240,250,240
160.          240 X=-BT
161.              Z=-BR
162.              RETURN
163.       C
164.       C      TRANSFORMS FIELD TO GEODETIC DIRECTIONS
165.       C
166.          250 SIND=SINLA*ST-SQRT(COSLA2)*CT
167.              COSD=SQRT(1.0-SIND**2)
168.              X=-BT*COSD-BR*SIND
169.              Z=BT*SIND-BR*COSD
170.              RETURN
171.       C
172.          260 FORMAT (2I1,1X,F6.1,10A6,A3)
173.          270 FORMAT (2I3,5X,6HEPOCH ,F7.1,5X10A6,A3)
174.          280 FORMAT (2I3,6F11.4)
175.          290 FORMAT (6H0 N  M,6X,1HG,10X,1HH,9X,2HGT,9X,2HHT,8X,3HGTT8X,3HHTT//
176.             1)
177.          300 FORMAT (2I3,6F11.4)
178.          310 FORMAT (2I3,F11.4,11X,F11.4,11XF11.4)
179.          320 FORMAT (///)
```

```
C
      END
      SUBROUTINE FIELD
      COMMON /NASA/ G(18,18)
      COMMON /FLDCOM/ ST,CT,SPH,CPH,R,NMAX,BT,BP,BR,B
      DIMENSION P(18,18), DP(18,18), CONST(18,18), SP(18), CP(18), FN(18
     1), FM(18)
      DATA P(1,1)/0./
      IF (P(1,1).EQ.1.0) GO TO 120
      P(1,1)=1.
      DP(1,1)=0.
      SP(1)=0.
      CP(1)=1.
      DO 110 N=2,18
         FN(N)=N
      DO 110 M=1,N
         FM(M)=M-1
  110 CONST(N,M)=FLOAT((N-2)**2-(M-1)**2)/FLOAT((2*N-3)*(2*N-5))
  120 SP(2)=SPH
      CP(2)=CPH
      DO 130 M=3,NMAX
         SP(M)=SP(2)*CP(M-1)+CP(2)*SP(M-1)
  130 CP(M)=CP(2)*CP(M-1)-SP(2)*SP(M-1)
      AOR=6371.0/R
      AR=AOR**2
      BT=0.
      BP=0.
      BR=0.
      DO 190 N=2,NMAX
         AR=AOR*AR
      DO 190 M=1,N
         IF (N-M) 150,140,150
  140    P(N,N)=ST*P(N-1,N-1)
         DP(N,N)=ST*DP(N-1,N-1)+CT*P(N-1,N-1)
         GO TO 160
  150    P(N,M)=CT*P(N-1,M)-CONST(N,M)*P(N-2,M)
         DP(N,M)=CT*DP(N-1,M)-ST*P(N-1,M)-CONST(N,M)*DP(N-2,M)
  160    PAR=P(N,M)*AR
         IF (M.EQ.1) GO TO 170
         TEMP=G(N,M)*CP(M)+G(M-1,N)*SP(M)
         BP=BP-(G(N,M)*SP(M)-G(M-1,N)*CP(M))*FM(M)*PAR
         GO TO 180
  170    TEMP=G(N,M)*CP(M)
         BP=BP-(G(N,M)*SP(M))*FM(M)*PAR
  180    BT=BT+TEMP*DP(N,M)*AR
  190 BR=BR-TEMP*FN(N)*PAR
      BP=BP/ST
      B=SQRT(BT*BT+BP*BP+BR*BR)
      RETURN
C
      END
```

0 N	0 M	EPOCH G	1980.0 H	GT	19 HT	IGR GTT	COEFCIEN HTT
2	1	-29988.0000		22.4000		0.0	
2	2	-1957.0000	5606.0000	11.3000	-15.9000	0.0	0.0
3	1	-1997.0000		-18.3000		0.0	
3	2	3028.0000	-2129.0000	3.2000	-12.7000	0.0	0.0
3	3	1662.0000	-199.0000	7.0000	-25.2000	0.0	0.0
4	1	1279.0000		0.0		0.0	
4	2	-2181.0000	-335.0000	-6.5000	0.2000	0.0	0.0
4	3	1251.0000	271.0000	-0.7000	2.7000	0.0	0.0
4	4	833.0000	-252.0000	1.0000	-7.9000	0.0	0.0
5	1	938.0000		-1.4000		0.0	
5	2	783.0000	212.0000	-1.4000	4.6000	0.0	0.0
5	3	398.0000	-257.0000	-8.2000	1.6000	0.0	0.0
5	4	-419.0000	53.0000	-1.8000	2.9000	0.0	0.0
5	5	199.0000	-298.0000	-5.0000	0.4000	0.0	0.0
6	1	-219.0000		1.5000		0.0	
6	2	357.0000	46.0000	0.4000	1.8000	0.0	0.0
6	3	261.0000	149.0000	-0.8000	-0.4000	0.0	0.0
6	4	-74.0000	-150.0000	-3.3000	0.0	0.0	0.0
6	5	-162.0000	-78.0000	1.3000	1.4000	0.0	0.0
6	6	-48.0000	92.0000	1.4000	2.1000	0.0	0.0
7	1	49.0000		0.4000		0.0	
7	2	65.0000	-15.0000	0.0	-0.5000	0.0	0.0
7	3	42.0000	93.0000	3.4000	-1.4000	0.0	0.0
7	4	-192.0000	71.0000	0.8000	0.0	0.0	0.0
7	5	4.0000	-43.0000	0.8000	-1.6000	0.0	0.0
7	6	14.0000	-2.0000	0.3000	0.5000	0.0	0.0
7	7	-108.0000	17.0000	-0.1000	0.0	0.0	0.0
8	1	70.0000		-1.0000		0.0	
8	2	-59.0000	-83.0000	-0.8000	-0.4000	0.0	0.0
8	3	2.0000	-28.0000	0.4000	0.4000	0.0	0.0
8	4	20.0000	-5.0000	0.5000	0.2000	0.0	0.0
8	5	-13.0000	16.0000	1.6000	1.4000	0.0	0.0
8	6	1.0000	18.0000	0.1000	-0.5000	0.0	0.0
8	7	11.0000	-23.0000	0.1000	-0.1000	0.0	0.0
8	8	-2.0000	-10.0000	0.0	1.1000	0.0	0.0
9	1	20.0000		0.8000		0.0	
9	2	7.0000	7.0000	-0.2000	-0.1000	0.0	0.0
9	3	1.0000	-18.0000	-0.3000	-0.7000	0.0	0.0
9	4	-11.0000	4.0000	0.3000	0.0	0.0	0.0
9	5	-7.0000	-22.0000	-0.8000	-0.8000	0.0	0.0
9	6	4.0000	9.0000	-0.2000	0.2000	0.0	0.0
9	7	3.0000	16.0000	0.7000	0.2000	0.0	0.0
9	8	7.0000	-13.0000	-0.3000	-1.1000	0.0	0.0
9	9	-1.0000	-15.0000	1.2000	0.8000	0.0	0.0
10	1	6.0000		0.0		0.0	
10	2	11.0000	-21.0000	0.0	0.0	0.0	0.0
10	3	2.0000	16.0000	0.0	0.0	0.0	0.0
10	4	-12.0000	9.0000	0.0	0.0	0.0	0.0
10	5	9.0000	-5.0000	0.0	0.0	0.0	0.0
10	6	-3.0000	-7.0000	0.0	0.0	0.0	0.0
10	7	-1.0000	9.0000	0.0	0.0	0.0	0.0
10	8	7.0000	10.0000	0.0	0.0	0.0	0.0
10	9	1.0000	-6.0000	0.0	0.0	0.0	0.0
10	10	-5.0000	2.0000	0.0	0.0	0.0	0.0
11	1	-3.0000		0.0		0.0	
11	2	-4.0000	1.0000	0.0	0.0	0.0	0.0
11	3	2.0000	1.0000	0.0	0.0	0.0	0.0
11	4	-5.0000	2.0000	0.0	0.0	0.0	0.0
11	5	-2.0000	5.0000	0.0	0.0	0.0	0.0
11	6	5.0000	-4.0000	0.0	0.0	0.0	0.0
11	7	3.0000	-1.0000	0.0	0.0	0.0	0.0
11	8	1.0000	-2.0000	0.0	0.0	0.0	0.0
11	9	2.0000	4.0000	0.0	0.0	0.0	0.0
11	10	3.0000	-1.0000	0.0	0.0	0.0	0.0
11	11	-5.0000	-6.0000	0.0	0.0	0.0	0.0

APPENDIX 3: DATA TABLES

(1)

DATE	TIME	LONGITUDE	LATITUDE	FIELD	IGRF	RESIDUAL	INC	DEC
AUGUST 21	18.83	-81.8046	40.1907	56260.0	56224.1	35.9	69.8200	-5.5262
AUGUST 21	19.00	-81.8165	40.2306	56186.2	56243.9	-57.7	69.8515	-5.5302
AUGUST 21	19.08	-81.8153	40.2380	56208.2	56247.4	-39.2	69.8572	-5.5341
AUGUST 21	19.23	-81.8031	40.2339	56212.4	56244.2	-31.8	69.8536	-5.5435
AUGUST 21	19.42	-81.7993	40.2396	56284.5	56246.7	37.8	69.8580	-5.5490
AUGUST 21	19.48	-81.8071	40.2413	56246.3	56248.2	-1.9	69.8595	-5.5426
AUGUST 21	19.62	-81.8150	40.2463	56241.5	56251.3	-9.8	69.8636	-5.5374
AUGUST 21	19.75	-81.8169	40.2513	56197.1	56253.8	-56.7	69.8676	-5.5375
AUGUST 21	20.00	-81.8299	40.2435	56206.7	56251.2	-44.5	69.8618	-5.5230
AUGUST 22	14.50	-81.7855	40.1713	56191.4	56213.3	-21.9	69.8044	-5.5362
AUGUST 22	14.57	-81.7885	40.1689	56216.4	56211.4	5.0	69.8019	-5.5338
AUGUST 22	14.83	-81.7980	40.1547	56157.3	56205.5	-48.2	69.7910	-5.5201
AUGUST 22	15.00	-81.8391	40.1876	56194.4	56224.7	-30.3	69.8178	-5.4954
AUGUST 22	15.12	-81.8430	40.1943	56229.9	56228.1	1.8	69.8232	-5.4943
AUGUST 22	15.40	-81.8441	40.1997	56146.8	56230.9	-84.1	69.8274	-5.4954
AUGUST 22	15.50	-81.8430	40.2038	56198.2	56232.7	-34.5	69.8305	-5.4978
AUGUST 22	15.62	-81.8310	40.2099	56259.7	56234.4	25.3	69.8350	-5.5109
AUGUST 22	16.00	-81.8036	40.2047	56240.2	56229.6	10.6	69.8302	-5.5335
AUGUST 22	16.32	-81.7839	40.1990	56243.3	56225.2	18.1	69.8251	-5.5490
AUGUST 22	16.50	-81.7855	40.2088	56268.3	56229.9	38.4	69.8328	-5.5512
AUGUST 22	16.58	-81.7967	40.2090	56338.0	56231.0	107.0	69.8333	-5.5413
AUGUST 22	16.67	-81.7928	40.2185	56195.0	56235.2	-40.2	69.8406	-5.5483

(2)

DATE	TIME	LONGITUDE	LATITUDE	FIELD	IGRF	RESIDUAL	INC	DEC
AUGUST 23	14.08	-81.8064	40.1360	56224.3	56197.4	26.9	69.7767	-5.5057
AUGUST 23	14.17	-81.8015	40.1401	56281.3	56198.9	82.4	69.7798	-5.5116
AUGUST 23	14.23	-81.7891	40.1376	56153.7	56196.6	-42.9	69.7775	-5.5218
AUGUST 23	14.33	-81.7695	40.1372	56180.0	56194.7	-14.7	69.7766	-5.5392
AUGUST 23	14.57	-81.7713	40.1502	56166.0	56201.1	-35.1	69.7868	-5.5424
AUGUST 23	14.75	-81.7636	40.1645	56152.0	56207.2	-55.2	69.7977	-5.5545
AUGUST 23	14.92	-81.7716	40.1659	56197.3	56208.5	-11.2	69.7990	-5.5478
30 — AUGUST 23	14.98	-81.7860	40.1556	56172.0	56204.9	-32.9	69.7915	-5.5311
AUGUST 23	15.17	-81.7650	40.1728	56180.0	56211.2	-31.2	69.8042	-5.5563
AUGUST 23	15.33	-81.7512	40.1771	56229.0	56211.9	17.1	69.8071	-5.5702
AUGUST 23	15.50	-81.7468	40.1805	56224.0	56213.1	10.9	69.8097	-5.5754
AUGUST 23	15.65	-81.7364	40.1889	56235.0	56216.2	18.8	69.8159	-5.5879
AUGUST 23	15.83	-81.7662	40.1900	56241.0	56219.4	21.6	69.8176	-5.5616
AUGUST 23	16.00	-81.7529	40.2025	56251.3	56224.1	27.2	69.8269	-5.5781
AUGUST 23	16.12	-81.7838	40.2034	56264.0	56227.2	36.8	69.8286	-5.5508
AUGUST 23	16.25	-81.7754	40.1962	56259.3	56223.2	36.1	69.8228	-5.5557
AUGUST 23	16.32	-81.7665	40.1974	56259.0	56223.0	36.0	69.8234	-5.5640
40 — AUGUST 23	16.42	-81.7665	40.2034	56224.3	56225.7	-1.4	69.8280	-5.5662
AUGUST 23	16.92	-81.7042	40.1876	56241.0	56212.7	28.3	69.8139	-5.6162
AUGUST 23	17.08	-81.6925	40.1841	56234.0	56210.1	23.9	69.8108	-5.6254
AUGUST 23	17.25	-81.6875	40.1796	56236.0	56207.4	28.6	69.8072	-5.6282
AUGUST 23	17.32	-81.6954	40.1711	56228.3	56204.1	24.2	69.8008	-5.6180
AUGUST 23	17.50	-81.6878	40.1658	56234.0	56201.0	33.0	69.7965	-5.6228
AUGUST 23	17.58	-81.6868	40.1596	56218.3	56197.9	20.4	69.7916	-5.6214
AUGUST 23	17.65	-81.6945	40.1575	56249.3	56197.6	51.7	69.7902	-5.6137
AUGUST 23	17.80	-81.7004	40.1480	56249.7	56193.6	56.1	69.7830	-5.6050
AUGUST 23	17.92	-81.7109	40.1467	56240.0	56193.9	46.1	69.7823	-5.5951
50 — AUGUST 23	18.00	-81.7108	40.1406	56232.0	56191.1	40.9	69.7776	-5.5929
AUGUST 23	18.15	-81.7196	40.1265	56284.7	56185.2	99.5	69.7668	-5.5799
AUGUST 23	18.25	-81.7278	40.1343	56249.7	56189.7	60.0	69.7731	-5.5754
AUGUST 23	18.33	-81.7388	40.1345	56246.7	56190.8	55.9	69.7736	-5.5656
AUGUST 23	18.48	-81.7326	40.1490	56235.0	56196.9	38.1	69.7847	-5.5765
AUGUST 23	18.58	-81.7253	40.1572	56243.7	56200.2	43.5	69.7909	-5.5861
AUGUST 23	18.75	-81.7285	40.1742	56283.0	56208.5	74.5	69.8042	-5.5895
AUGUST 23	18.83	-81.7262	40.1809	56260.0	56211.4	48.6	69.8094	-5.5940
AUGUST 23	18.92	-81.7216	40.1924	56279.0	56216.5	62.5	69.8182	-5.6024
AUGUST 23	19.00	-81.7102	40.1912	56261.3	56214.9	46.4	69.8169	-5.6122

(3)

DATE	TIME	LONGITUDE	LATITUDE	FIELD	IGRF	RESIDUAL	INC	DEC
AUGUST 24	14.50	-81.8508	40.1770	56299.7	56220.6	79.1	69.8099	-5.4810
AUGUST 24	14.83	-81.8498	40.1576	56183.2	56211.4	-28.2	69.7948	-5.4748
AUGUST 24	15.07	-81.8515	40.1435	56254.8	56204.9	49.9	69.7839	-5.4681
AUGUST 24	15.25	-81.8698	40.1512	56246.2	56210.2	36.0	69.7904	-5.4546
AUGUST 24	15.50	-81.8790	40.1397	56236.8	56205.6	31.2	69.7817	-5.4421
AUGUST 24	15.67	-81.8824	40.1352	56302.0	56203.8	98.2	69.7782	-5.4374
AUGUST 24	15.83	-81.8803	40.1307	56289.9	56201.5	88.4	69.7747	-5.4377
AUGUST 24	17.17	-81.9122	40.1860	56123.3	56230.2	-106.9	69.8186	-5.4293
AUGUST 24	17.25	-81.9201	40.1887	56136.3	56232.3	-96.0	69.8210	-5.4232
AUGUST 24	17.33	-81.9325	40.1918	56147.9	56234.8	-86.9	69.8237	-5.4132
AUGUST 24	17.58	-81.9315	40.1818	56212.0	56229.9	-17.9	69.8159	-5.4105
AUGUST 24	17.43	-81.9341	40.1708	56171.2	56225.1	-53.9	69.8073	-5.4041
AUGUST 24	17.92	-81.9161	40.1681	56102.2	56222.3	-120.1	69.8048	-5.4193
AUGUST 24	18.00	-81.9043	40.1799	56138.5	56226.7	-88.2	69.8137	-5.4342
AUGUST 24	18.17	-81.8986	40.1884	56118.3	56230.3	-112.0	69.8201	-5.4424
AUGUST 24	18.25	-81.9141	40.1992	56121.7	56236.8	-115.1	69.8289	-5.4325
AUGUST 24	18.33	-81.9232	40.2079	56138.6	56241.6	-103.0	69.8360	-5.4275
AUGUST 24	18.42	-81.9174	40.2093	56149.2	56241.7	-92.5	69.8369	-5.4332
AUGUST 24	18.55	-81.8911	40.2438	56058.4	56255.7	-197.3	69.8630	-5.4694
AUGUST 24	18.67	-81.8939	40.2371	56022.0	56252.9	-230.9	69.8580	-5.4645
AUGUST 25	14.98	-81.9452	40.1708	56295.7	56226.0	69.7	69.8076	-5.3942
AUGUST 25	15.13	-81.9517	40.1809	56244.7	56231.2	13.4	69.8157	-5.3921
AUGUST 25	15.25	-81.9516	40.1873	56256.7	56234.4	22.3	69.8207	-5.3945
AUGUST 25	15.40	-31.9606	40.2032	56265.9	56242.6	23.3	69.8333	-5.3922
AUGUST 25	15.58	-81.9820	40.1893	56279.8	56237.9	41.9	69.8231	-5.3680
AUGUST 25	15.75	-81.9882	40.1789	56215.8	56233.5	-17.7	69.8151	-5.3586
AUGUST 25	15.83	-81.9771	40.1803	56250.3	56233.2	17.1	69.8159	-5.3691
AUGUST 25	15.92	-81.9612	40.1798	56250.1	56231.6	18.5	69.8152	-5.3832
AUGUST 25	15.96	-81.9583	40.1762	56281.5	56229.6	51.9	69.8122	-5.3844
AUGUST 25	16.33	-81.9318	40.1563	56287.4	56218.0	69.4	69.7960	-5.4009
AUGUST 25	16.58	-81.9464	40.1514	56326.0	56216.8	109.2	69.7926	-5.3860
AUGUST 25	16.67	-81.9534	40.1379	56420.4	56211.2	209.2	69.7822	-5.3749
AUGUST 25	16.73	-81.9648	40.1300	56406.3	56212.7	193.6	69.7834	-5.3650
AUGUST 25	16.92	-81.9634	40.1445	56377.7	56215.1	162.6	69.7876	-5.3683
AUGUST 25	17.00	-81.9562	40.1553	56327.5	56219.7	107.8	69.7959	-5.3787
AUGUST 25	17.07	-81.9673	40.1544	56275.4	56220.2	55.2	69.7954	-5.3684
AUGUST 25	17.17	-81.9926	40.1523	56257.9	56221.4	36.5	69.7945	-5.3450
AUGUST 25	17.50	-81.9909	40.1663	56345.6	56227.9	117.7	69.8054	-5.3516
AUGUST 25	17.67	-81.9814	40.1660	56297.6	56227.0	70.6	69.8049	-5.3600
AUGUST 25	17.75	-81.9677	40.1631	56298.6	56224.4	74.2	69.8023	-5.3713
AUGUST 25	17.92	-81.9402	40.1587	56274.7	56219.8	54.9	69.7981	-5.3943

DATE	TIME	LONGITUDE	LATITUDE	FIELD	IGRF	RESIDUAL	INC	DEC
AUGUST 31	14.75	-81.8571	40.1971	56128.8	56228.8	-100.0	69.[illegible]	-5.4853
AUGUST 31	14.92	-81.8604	40.2186	56126.4	56239.2	-112.8	69.8411	-5.4902
AUGUST 31	15.00	-81.8531	40.2179	56088.2	56238.2	-150.0	69.8403	-5.4965
AUGUST 31	15.08	-81.8348	40.2202	56125.8	56237.7	-111.9	69.8416	-5.5137
AUGUST 31	15.13	-81.8343	40.2300	56258.1	56242.2	15.9	69.8492	-5.5178
AUGUST 31	15.18	-81.8518	40.2337	56110.2	56245.4	-135.2	69.8526	-5.5035
AUGUST 31	16.92	-81.8811	40.2314	56176.8	56246.9	-70.1	69.8516	-5.4764
AUGUST 31	17.00	-81.8825	40.2172	56102.5	56240.5	-138.0	69.8406	-5.4699
AUGUST 31	17.08	-81.8861	40.2067	56051.5	56235.8	-184.3	69.8325	-5.4628
AUGUST 31	17.20	-81.8936	40.2103	56074.4	56238.1	-163.7	69.8355	-5.4574
AUGUST 31	17.32	-81.8927	40.2401	56140.7	56252.1	-111.4	69.8587	-5.4692
AUGUST 31	17.45	-81.8736	40.2477	56289.3	56254.1	35.2	69.8641	-5.4891
SEPT. 3	15.42	-81.7960	40.2816	56293.7	56262.2	31.5	69.8875	-5.5725
SEPT. 3	15.50	-81.7896	40.2801	56265.7	56260.9	4.8	69.8862	-5.5777
SEPT. 3	15.53	-81.7957	40.2770	56206.9	56259.8	-52.9	69.8839	-5.5710
SEPT. 3	15.58	-81.8068	40.2759	56368.4	56260.3	108.1	69.8834	-5.5606
SEPT. 3	15.67	-81.8114	40.2707	56243.8	56258.4	-14.6	69.8795	-5.5546
SEPT. 3	15.75	-81.8144	40.2657	56258.8	56256.1	2.7	69.8757	-5.5500
SEPT. 3	15.83	-81.8155	40.2581	56220.1	56252.7	-32.6	69.8698	-5.5463
SEPT. 3	16.00	-81.7946	40.2431	56247.2	56243.8	3.4	69.8575	-5.5594
SEPT. 3	16.20	-81.7834	40.2517	56256.8	56246.9	9.9	69.8639	-5.5727
SEPT. 3	16.25	-81.7785	40.2622	56271.9	56251.3	20.6	69.8719	-5.5810
SEPT. 3	16.28	-81.7738	40.2643	56230.8	56251.9	-21.1	69.8734	-5.5860
SEPT. 3	16.33	-81.7640	40.2637	56276.3	56250.7	25.6	69.8726	-5.5945
SEPT. 3	16.42	-81.7592	40.2635	56263.5	56250.2	13.3	69.8724	-5.5987
SEPT. 3	16.50	-81.7558	40.2555	56229.7	56246.2	-16.5	69.8660	-5.5988
SEPT. 3	16.58	-81.7698	40.2706	56268.4	56254.6	13.8	69.8782	-5.5919
SEPT. 3	17.17	-81.7072	40.2725	56156.5	56249.9	-93.4	69.8778	-5.6487
SEPT. 3	17.33	-81.7174	40.2667	56179.6	56248.1	-68.5	69.8735	-5.6374
SEPT. 3	17.58	-81.7291	40.2467	56183.1	56239.8	-56.7	69.8584	-5.6195
SEPT. 3	17.67	-81.7437	40.2424	56222.8	56239.0	-16.2	69.8555	-5.6048
SEPT. 3	17.83	-81.7317	40.2321	56210.0	56233.0	-23.0	69.8471	-5.6117
SEPT. 3	18.00	-81.7181	40.2359	56142.8	56233.7	-90.9	69.8496	-5.6253
SEPT. 3	18.07	-81.7105	40.2416	56112.1	56235.6	-123.5	69.8538	-5.6343
SEPT. 3	18.18	-81.7080	40.2486	56121.7	56238.8	-117.1	69.8592	-5.6391
SEPT. 3	18.25	-81.6918	40.2513	56131.3	56238.6	-107.3	69.8608	-5.6547
SEPT. 3	18.33	-81.6856	40.2483	56123.6	56236.7	-113.1	69.8583	-5.6591
SEPT. 3	18.42	-81.6736	40.2133	56151.2	56219.0	-67.8	69.8307	-5.6568
SEPT. 3	18.50	-81.6596	40.2116	56129.8	56216.9	-87.1	69.8290	-5.6687
SEPT. 3	18.65	-81.6312	40.2132	56153.4	56215.1	-61.7	69.8293	-5.6947
SEPT. 3	18.75	-81.6264	40.2510	56111.0	56232.6	-121.6	69.8585	-5.7131
SEPT. 3	19.03	-81.6567	40.2637	56079.8	56241.1	-161.3	69.8694	-5.6907
SEPT. 3	19.58	-81.7372	40.2219	56171.4	56228.8	-57.4	69.8394	-5.6030
SEPT. 3	19.67	-81.7666	40.2203	56251.3	56230.6	20.7	69.8389	-5.5761
SEPT. 3	19.73	-81.7755	40.2209	56263.6	56231.7	31.9	69.8397	-5.5684

(5)

DATE		TIME	LONGITUDE	LATITUDE	FIELD	IGRF	RESIDUAL	INC	DEC
SEPT.	6	14.50	-81.8669	40.2859	56205.9	56269.4	-63.5	69.8921	-5.5116
SEPT.	6	14.83	-81.8267	40.3086	56234.0	56276.4	-42.4	69.9086	-5.5561
SEPT.	6	14.97	-81.8157	40.3075	56226.3	56275.0	-48.7	69.9074	-5.5656
SEPT.	6	15.07	-81.8097	40.3058	56223.0	56273.6	-50.6	69.9059	-5.5704
150 ← SEPT.	6	15.15	-81.8022	40.3040	56207.1	56272.2	-65.1	69.9043	-5.5764
SEPT.	6	15.23	-81.7931	40.3054	56236.2	56272.0	-35.8	69.9052	-5.5851
SEPT.	6	15.38	-81.7734	40.3231	56221.7	56278.5	-56.8	69.9183	-5.6094
SEPT.	6	15.50	-81.7839	40.3197	56192.9	56277.9	-85.0	69.9160	-5.5987
SEPT.	6	15.67	-81.7793	40.3353	56223.2	56284.9	-61.7	69.9280	-5.6086
SEPT.	6	15.78	-81.7901	40.3182	56222.2	56277.8	-55.6	69.9150	-5.5926
SEPT.	6	18.58	-81.8178	40.2982	56226.9	56270.7	-43.8	69.9003	-5.5602
SEPT.	6	18.63	-81.8173	40.2941	56252.4	56268.8	-16.4	69.8970	-5.5592
SEPT.	6	18.83	-81.7999	40.2940	56177.9	56267.2	-89.3	69.8964	-5.5748
SEPT.	6	19.00	-81.7855	40.2924	56234.1	56265.2	-31.1	69.8948	-5.5871
160 ← SEPT.	6	19.17	-81.7514	40.3049	56135.0	56268.1	-133.1	69.9035	-5.6224
SEPT.	6	19.25	-81.7608	40.3073	56134.9	56270.0	-135.1	69.9056	-5.6148
SEPT.	6	19.33	-81.7787	40.3059	56107.0	56270.9	-163.9	69.9051	-5.5982
SEPT.	6	19.50	-81.7587	40.2942	56179.5	56263.6	-84.1	69.8954	-5.6118
SEPT.	6	19.67	-81.7367	40.2898	56131.5	56259.6	-128.1	69.8913	-5.6300
SEPT.	6	19.75	-81.7141	40.2928	56110.7	56259.0	-148.3	69.8929	-5.6513
SEPT.	6	19.83	-81.7029	40.3059	56120.7	56264.2	-143.5	69.9023	-5.6662
SEPT.	6	19.90	-81.7295	40.3187	56110.0	56272.6	-162.6	69.9136	-5.6472

(6)

DATE		TIME	LONGITUDE	LATITUDE	FIELD	IGRF	RESIDUAL	INC	DEC
SEPT.	7	12.17	-81.7448	40.3464	56244.0	56287.0	-43.0	69.9355	-5.6437
SEPT.	7	12.25	-81.7535	40.3456	56006.0	56287.4	-281.4	69.9352	-5.6356
170 ← SEPT.	7	12.33	-81.7487	40.3374	56069.4	56283.1	-213.7	69.9287	-5.6369
SEPT.	7	12.42	-81.7370	40.3281	56109.4	56277.6	-168.2	69.9211	-5.6439
SEPT.	7	12.58	-81.7529	40.3277	56120.4	56278.8	-158.4	69.9213	-5.6295
SEPT.	7	12.83	-81.7426	40.3696	56102.5	56297.6	-195.1	69.9535	-5.6544
SEPT.	7	12.92	-81.7516	40.3678	56103.6	56297.6	-194.0	69.9523	-5.6456
SEPT.	7	13.00	-81.7565	40.3718	56101.7	56299.9	-198.2	69.9556	-5.6427
SEPT.	7	13.17	-81.7638	40.3571	56098.5	56293.6	-195.1	69.9444	-5.6307
SEPT.	7	13.25	-81.7657	40.3525	56106.0	56291.7	-185.7	69.9409	-5.6273
SEPT.	7	13.30	-81.7601	40.3543	56101.0	56292.0	-191.0	69.9422	-5.6330
SEPT.	7	13.67	-81.6910	40.3237	56120.4	56271.4	-151.0	69.9163	-5.6836
180 ← SEPT.	7	13.75	-81.6899	40.3268	56128.6	56272.8	-144.2	69.9186	-5.6857
SEPT.	7	13.92	-81.7020	40.3401	56140.5	56280.1	-139.6	69.9293	-5.6798
SEPT.	7	14.05	-81.7109	40.3394	56134.2	56280.6	-146.4	69.9291	-5.6716
SEPT.	7	14.13	-81.7206	40.3386	56123.0	56281.1	-158.1	69.9287	-5.6625
SEPT.	7	14.33	-81.7147	40.3225	56150.0	56273.0	-123.0	69.9161	-5.6618
SEPT.	7	14.50	-81.7047	40.3204	56145.0	56271.2	-126.2	69.9142	-5.6701
SEPT.	7	14.58	-81.6981	40.3142	56144.9	56267.7	-122.8	69.9091	-5.6737
SEPT.	7	14.75	-81.6812	40.3532	56151.7	56284.4	-132.7	69.9389	-5.7034
SEPT.	7	14.92	-81.6629	40.3568	56132.7	56284.4	-151.7	69.9411	-5.7212
SEPT.	7	15.00	-81.6674	40.3478	56141.3	56280.7	-139.4	69.9342	-5.7138
190 ← SEPT.	7	15.08	-81.6654	40.3380	56175.1	56275.9	-100.8	69.9266	-5.7120
SEPT.	7	15.17	-81.6740	40.3385	56176.3	56276.9	-100.6	69.9272	-5.7044
SEPT.	7	15.25	-81.6832	40.3407	56172.1	56278.7	-106.6	69.9292	-5.6969
SEPT.	7	15.50	-81.6850	40.2840	56167.8	56252.3	-84.5	69.8852	-5.6742
SEPT.	7	15.67	-81.6622	40.3069	56216.9	56261.0	-44.1	69.9023	-5.7032
SEPT.	7	15.75	-81.6623	40.3195	56171.4	56266.9	-95.5	69.9121	-5.7078
SEPT.	7	15.83	-81.6557	40.3105	56187.3	56262.2	-74.9	69.9049	-5.7103
SEPT.	7	15.92	-81.6510	40.2940	56191.5	56253.9	-62.4	69.8919	-5.7084
SEPT.	7	16.00	-81.6312	40.2881	56186.7	56249.4	-62.7	69.8868	-5.7239
SEPT.	7	16.25	-81.6237	40.3197	56194.3	56263.5	-69.2	69.9111	-5.7425
200 ← SEPT.	7	16.30	-81.6254	40.3223	56176.7	56264.9	-88.2	69.9131	-5.7420
SEPT.	7	16.33	-81.6370	40.3269	56196.8	56268.0	-71.2	69.9171	-5.7332
SEPT.	7	16.42	-81.6460	40.3330	56175.8	56271.8	-96.0	69.9220	-5.7275
SEPT.	7	16.50	-81.6473	40.3275	56184.0	56269.2	-85.2	69.9179	-5.7243
SEPT.	7	16.67	-81.6495	40.3175	56207.6	56264.9	-57.3	69.9101	-5.7185
SEPT.	8	14.50	-81.6195	40.3485	56126.0	56276.7	-150.7	69.9332	-5.7571
SEPT.	8	14.67	-81.6367	40.3497	56116.4	56278.8	-162.4	69.9347	-5.7421
SEPT.	8	14.83	-81.6342	40.3610	56123.7	56283.7	-160.0	69.9434	-5.7486
SEPT.	8	14.92	-81.6242	40.3664	56112.1	56285.4	-173.3	69.9473	-5.7596
SEPT.	8	15.00	-81.6170	40.3641	56124.1	56283.8	-159.7	69.9453	-5.7652
210 ← SEPT.	8	15.50	-81.7167	40.3822	56121.3	56301.0	-179.7	69.9624	-5.6824
SEPT.	8	15.58	-81.7270	40.3760	56070.5	56299.2	-228.7	69.9579	-5.6707
SEPT.	8	15.67	-81.7345	40.3783	56110.9	56300.8	-189.9	69.9600	-5.6649
SEPT.	8	15.83	-81.7279	40.3689	56153.1	56296.0	-142.9	69.9525	-5.6673
SEPT.	8	16.00	-81.6921	40.3650	56132.8	56291.0	-158.2	69.9483	-5.6980
SEPT.	8	16.25	-81.6821	40.3597	56086.5	56287.5	-201.0	69.9440	-5.7051
SEPT.	8	16.50	-81.7178	40.3607	56133.5	56291.2	-157.7	69.9458	-5.6734
SEPT.	8	16.67	-81.7056	40.3540	56152.5	56287.0	-134.5	69.9402	-5.6818
SEPT.	8	16.75	-81.7199	40.3488	56152.2	56285.9	-133.7	69.9366	-5.6670
SEPT.	8	16.78	-81.7301	40.3428	56126.4	56283.9	-157.5	69.9323	-5.6556
220 ← SEPT.	8	16.83	-81.7344	40.3550	56098.2	56290.0	-191.8	69.9419	-5.6563

(7)

DATE		TIME	LONGITUDE	LATITUDE	FIELD	IGRF	RESIDUAL	INC	DEC
SEPT.	9	14.17	-81.8478	40.3604	56299.6	56301.6	-2.0	69.9487	-5.5576
SEPT.	9	14.25	-81.8342	40.3667	56137.7	56303.4	-165.7	69.9532	-5.5722
SEPT.	9	14.33	-81.8274	40.3783	56158.7	56308.1	-149.4	69.9620	-5.5826
SEPT.	9	14.42	-81.8366	40.3890	56198.7	56314.0	-115.3	69.9706	-5.5783
SEPT.	9	14.50	-81.8384	40.4020	56199.5	56320.3	-120.8	69.9808	-5.5815
SEPT.	9	14.58	-81.8519	40.3761	56227.3	56309.3	-82.0	69.9611	-5.5598
SEPT.	9	14.75	-81.8562	40.3632	56205.4	56303.6	-98.2	69.9511	-5.5511
SEPT.	9	14.92	-81.8492	40.3568	56226.5	56300.0	-73.5	69.9460	-5.5550
SEPT.	9	15.00	-81.8459	40.3479	56203.6	56295.7	-92.1	69.9389	-5.5547
230 ← SEPT.	9	15.08	-81.8488	40.3404	56193.1	56292.3	-99.2	69.9332	-5.5493
SEPT.	9	15.17	-81.8593	40.3446	56219.4	56295.3	-75.9	69.9368	-5.5414
SEPT.	9	15.25	-81.8637	40.3307	56262.9	56289.0	-26.1	69.9261	-5.5323
SEPT.	9	15.30	-81.8644	40.3372	56210.7	56292.2	-81.5	69.9312	-5.5341
SEPT.	9	15.33	-81.8579	40.3266	56202.6	56286.6	-84.0	69.9227	-5.5360
SEPT.	9	15.50	-81.8720	40.3576	56240.4	56302.4	-62.0	69.9472	-5.5348
SEPT.	9	15.58	-81.8745	40.3654	56204.8	56306.4	-101.6	69.9533	-5.5355
SEPT.	9	15.75	-81.8708	40.3822	56211.3	56313.7	-102.4	69.9663	-5.5450
SEPT.	9	15.92	-81.8637	40.3121	56175.0	56280.3	-105.3	69.9117	-5.5254
SEPT.	9	16.00	-81.8719	40.2968	56250.5	56273.8	-23.3	69.9000	-5.5125
240 ← SEPT.	9	16.17	-81.8458	40.3258	56188.3	56285.2	-96.9	69.9217	-5.5466
SEPT.	9	16.25	-81.8310	40.3250	56155.7	56283.5	-127.8	69.9207	-5.5596
SEPT.	9	16.33	-81.8328	40.3218	56175.4	56282.2	-106.8	69.9183	-5.5568
SEPT.	9	16.42	-81.8349	40.3080	56232.6	56275.9	-43.3	69.9076	-5.5498
SEPT.	9	16.58	-81.8475	40.2961	56235.0	56271.4	-36.4	69.8988	-5.5341
SEPT.	9	16.75	-81.8378	40.3026	56208.5	56273.7	-65.2	69.9036	-5.5452
SEPT.	9	16.83	-81.8570	40.2930	56197.9	56270.7	-72.8	69.8966	-5.5244
SEPT.	9	17.08	-81.8046	40.3407	56142.3	56288.5	-146.2	69.9321	-5.5891
SEPT.	9	17.17	-81.8005	40.3424	56113.2	56289.0	-175.8	69.9333	-5.5934
SEPT.	9	17.25	-81.7970	40.3506	56140.6	56292.6	-152.0	69.9396	-5.5996
250 ← SEPT.	9	17.42	-81.7793	40.3353	56137.3	56283.8	-146.5	69.9272	-5.6099
SEPT.	9	17.50	-81.7772	40.3426	56144.8	56287.0	-142.2	69.9328	-5.6145
SEPT.	9	17.58	-81.7824	40.3579	56098.3	56294.6	-196.3	69.9448	-5.6155
SEPT.	9	17.67	-81.7943	40.3544	56133.3	56294.1	-160.8	69.9425	-5.6035
SEPT.	9	17.83	-81.8009	40.3632	56141.8	56298.7	-156.9	69.9495	-5.6008
SEPT.	9	17.92	-81.7934	40.3589	56137.8	56296.1	-158.3	69.9459	-5.6059
SEPT.	9	18.00	-81.8136	40.3511	56148.6	56294.3	-145.7	69.9404	-5.5849
SEPT.	9	18.08	-81.8136	40.3562	56116.0	56296.6	-180.6	69.9444	-5.5868
SEPT.	9	18.17	-81.8080	40.3548	56125.1	56295.5	-170.4	69.9432	-5.5913
SEPT.	9	18.33	-81.8277	40.3354	56124.5	56288.2	-163.7	69.9287	-5.5664
260 ← SEPT.	9	18.42	-81.8315	40.3432	56132.9	56292.2	-159.3	69.9348	-5.5659
SEPT.	9	18.50	-81.8227	40.3568	56133.0	56297.7	-164.7	69.9452	-5.5789
SEPT.	9	18.58	-81.8304	40.3571	56130.0	56298.5	-168.5	69.9456	-5.5720
SEPT.	9	18.83	-81.7817	40.3667	56136.9	56298.8	-161.9	69.9516	-5.6194
SEPT.	9	18.92	-81.7760	40.3649	56103.0	56297.4	-194.4	69.9501	-5.6239
SEPT.	9	19.00	-81.7928	40.3695	56105.1	56301.0	-195.9	69.9542	-5.6105
SEPT.	9	19.08	-81.7992	40.3712	56144.8	56302.4	-157.6	69.9556	-5.6053
SEPT.	9	19.17	-81.7927	40.3804	56160.6	56306.0	-145.4	69.9626	-5.6146

(9)

DATE	TIME	LONGITUDE	LATITUDE	FIELD	IGRF	RESIDUAL	INC	DEC
SEPT. 10	16.33	-81.8694	40.3982	56330.8	56321.3	9.5	69.9787	-5.5522
SEPT. 10	16.42	-81.8730	40.4041	56285.4	56324.3	-38.9	69.9834	-5.5512
270 ← SEPT. 10	16.50	-81.8687	40.4115	56410.2	56327.3	82.9	69.9890	-5.5578
SEPT. 10	16.67	-81.8593	40.4136	56353.0	56327.4	25.6	69.9903	-5.5670
SEPT. 10	16.75	-81.8645	40.4030	56332.7	56323.1	9.6	69.9823	-5.5584
SEPT. 10	16.92	-81.8687	40.4415	56535.7	56341.3	194.4	70.0122	-5.5690
SEPT. 10	17.08	-81.8723	40.4406	56575.5	56341.2	234.2	70.0116	-5.5654
SEPT. 10	17.17	-81.8728	40.4314	56523.3	56337.1	186.2	70.0045	-5.5615
SEPT. 10	17.33	-81.8632	40.4265	56435.7	56333.9	101.8	70.0005	-5.5684
SEPT. 10	17.42	-81.8418	40.4366	56333.5	56336.7	-3.2	70.0077	-5.5914
SEPT. 10	17.50	-81.8377	40.4435	56324.3	56339.5	-15.2	70.0129	-5.5976
SEPT. 10	17.67	-81.8241	40.4271	56277.0	56330.8	-53.8	69.9998	-5.6038
280 ← SEPT. 10	17.75	-81.8076	40.4167	56243.5	56324.4	-80.9	69.9912	-5.6147
SEPT. 10	17.83	-81.8104	40.4103	56212.0	56321.6	-109.6	69.9864	-5.6098
SEPT. 10	17.92	-81.8122	40.4030	56207.5	56318.4	-110.9	69.9808	-5.6055
SEPT. 10	18.00	-81.8341	40.4127	56302.4	56324.8	-22.4	69.9889	-5.5894
SEPT. 10	18.17	-81.8512	40.4222	56372.4	56330.8	41.6	69.9968	-5.5775
SEPT. 11	12.33	-81.8706	40.4586	56367.7	56349.5	18.2	70.0255	-5.5736
SEPT. 11	12.42	-81.8667	40.4684	56431.7	56353.8	77.9	70.0330	-5.5807
SEPT. 11	12.50	-81.8690	40.4734	56406.2	56356.3	49.9	70.0369	-5.5806
SEPT. 11	12.58	-81.8560	40.4726	56385.9	56354.7	31.2	70.0360	-5.5920
SEPT. 11	12.67	-81.8488	40.4624	56342.7	56349.5	-6.8	70.0279	-5.5947
290 ← SEPT. 11	12.75	-81.8473	40.4541	56357.9	56345.4	12.5	70.0214	-5.5930
SEPT. 11	12.83	-81.8706	40.4586	56367.7	56349.5	18.2	70.0255	-5.5736
SEPT. 11	12.92	-81.8611	40.4558	56403.3	56347.4	55.9	70.0231	-5.5811
SEPT. 11	13.08	-81.8068	40.4396	56177.3	56335.0	-157.7	70.0089	-5.6240
SEPT. 11	13.17	-81.8145	40.4326	56225.0	56332.5	-107.5	70.0037	-5.6145
SEPT. 11	13.25	-81.8239	40.4426	56265.5	56337.9	-72.4	70.0118	-5.6097
SEPT. 11	13.33	-81.8240	40.4550	56335.0	56343.7	-8.7	70.0214	-5.6143
SEPT. 11	13.42	-81.8025	40.4539	56196.4	56341.3	-144.9	70.0199	-5.6332
SEPT. 11	13.50	-81.7849	40.4313	56128.3	56329.3	-201.0	70.0018	-5.6406
SEPT. 11	13.58	-81.7822	40.4358	56159.7	56331.1	-171.4	70.0053	-5.6447
300 ← SEPT. 11	13.67	-81.7888	40.4244	56142.2	56326.3	-184.1	69.9966	-5.6345
SEPT. 11	13.75	-81.7868	40.4194	56141.3	56323.8	-182.5	69.9927	-5.6345
SEPT. 11	13.78	-81.7871	40.4120	56125.9	56320.3	-194.4	69.9870	-5.6314
SEPT. 11	13.83	-81.7814	40.4077	56120.2	56317.8	-197.6	69.9834	-5.6349
SEPT. 11	13.92	-81.7716	40.4232	56114.7	56324.2	-209.5	69.9952	-5.6496
SEPT. 11	14.00	-81.7741	40.4192	56108.0	56322.6	-214.6	69.9922	-5.6458
SEPT. 11	14.05	-81.7723	40.4127	56106.3	56319.3	-213.0	69.9870	-5.6450
SEPT. 11	14.08	-81.7687	40.4055	56113.8	56315.7	-201.9	69.9814	-5.6455
SEPT. 11	14.17	-81.7649	40.3974	56113.5	56311.5	-198.0	69.9750	-5.6460
SEPT. 11	14.25	-81.7725	40.3945	56107.0	56310.8	-203.8	69.9730	-5.6380
310 ← SEPT. 11	14.33	-81.7786	40.4000	56129.6	56314.0	-184.4	69.9774	-5.6346
SEPT. 11	14.42	-81.7896	40.3969	56151.9	56313.6	-161.7	69.9753	-5.6236
SEPT. 11	14.50	-81.8046	40.3959	56165.8	56314.5	-148.7	69.9750	-5.6097
SEPT. 11	14.53	-81.8032	40.3878	56135.3	56310.5	-175.2	69.9687	-5.6079
SEPT. 11	14.67	-81.7713	40.3849	56107.0	56306.2	-199.2	69.9655	-5.6355
SEPT. 11	14.75	-81.7673	40.3788	56067.9	56303.0	-235.1	69.9606	-5.6369
SEPT. 11	14.83	-81.7587	40.3870	56079.0	56306.0	-227.0	69.9667	-5.6476
SEPT. 11	14.88	-81.7523	40.3867	56047.5	56305.5	-258.0	69.9663	-5.6533
SEPT. 11	14.92	-81.7529	40.4085	56007.2	56315.6	-308.4	69.9831	-5.6609
SEPT. 11	14.96	-81.7550	40.4013	56078.0	56312.6	-234.6	69.9777	-5.6563
1076 320 SEPT. 11	15.00	-81.7543	40.3957	56112.1	56309.7	-197.6	69.9733	-5.6549